

2

AD-A252 440



DTIC  
ELECTE  
JUL 6 1992  
S C D

**US-Japan Seminar on Magnetic Multilayered Structures**

**Poipu Beach, Kauai, Hawaii**

**May 15-17, 1992**

*N00014-92-J-1386*

Sponsored by

National Science Foundation

Japan Society for the Promotion of Science

Office of Naval Research

and

Faculty of Arts and Science of New York University

DISTRIBUTION STATEMENT A  
Approved for public release;  
distribution unlimited

92-16326



92 6 19 039

# *Program*

for

## US-Japan Seminar on Magnetic Multilayered Structures

Friday, May 15, 1992

### **Structural properties and characterization of multilayered structures.**

- 8:30 am H. Fujimori, "Advancement in soft magnetic materials by means of multilayering".
- 9:15 am R. Yamamoto, "Elastic moduli of metallic multilayered films measured by Brillouin Scattering method".
- 10:00 am Y. Fujii, "Structural aspects of superlattices under high pressure".
- 10:45 am Coffee
- 11:15 am C.M. Falco, "Structural influence on the magnetic anisotropy of Co/Pd superlattices".
- 12:00 noon C.P. Flynn, "Low dimensional magnetic and structural effects in single crystals grown by molecular beam epitaxy".
- 12:45 pm Recess for lunch
- 1:45 pm Y. Endoh, "Polarized neutron reflection and diffraction from magnetic superlattices".
- 2:30 pm H. Yasuoka, "Nuclear Magnetic Resonance studies of magnetic multilayers".
- 3:15 pm M. Takahashi, "Thin film growth on the substrate excited by SAW and in-situ SAW propagation property".
- 4:00 pm M. Doyama, "Physical properties of multilayered FCC-Fe/Cu(100) and Fe/Cu(111) artificial lattice".

Saturday, May 16, 1992

**Magnetoresistance**

- 8:30 am T. Shinjo, "Magnetic structure and magneto-transport properties of multilayers with two magnetic components".
- 9:15 am S. Tsunashima, "Giant magnetoresistance in FeNiCo/Cu multilayers".
- 10:00 am T. Miyazaki, "Magnetoresistance of 82Ni-Fe/Al-Al<sub>2</sub>O<sub>3</sub>/Co junction".
- 10:45 am Coffee
- 11:15 am W.P. Pratt, Jr., "Magnetoresistance for currents *perpendicular* to the plane of the multilayers".
- 12 noon S.S.P. Parkin, "Giant magnetoresistance in magnetic multilayers and sandwiches".
- 12:45 pm Recess for lunch
- 1:45 pm S. Maekawa, "Theory of transport properties in magnetic superlattices".
- 2:30 pm L.M. Falicov, "Boltzmann equation approach to the negative magnetoresistance of ferromagnetic normal metallic multilayers".
- 3:15 pm P.M. Levy, "Magnetoresistivity of multilayers for current in plane and perpendicular to the plane of the layers".



Statement A per telecon Dr. Larry Cooper  
ONR/Code 1114  
Arlington, VA 22217-5000

NWW 6/29/92

Accession For	
NO. 1114	<input checked="" type="checkbox"/>
BY: SA	<input type="checkbox"/>
DATE: 6/29/92	<input type="checkbox"/>
Distribution/	
Availability Codes	
Dist	Special
A-1	

Sunday May 17, 1992

**Interlayer Coupling**

8:30 am S.D. Bader, "Magneto-optic characterizations of superlattices and wedged sandwiches with oscillatory interlayer magnetic coupling".

9:15 am D.T. Pierce, "Oscillations of the exchange coupling in Fe/Cr/Fe(100) and Fe/Ag/Fe(100)".

10:00 am G.A. Prinz, "Strong temperature dependence of the 90° coupling in Fe/Al/Fe(100) magnetic trilayers".

10:45 am Coffee

11:15 am K. Takanashi, "Ferrimagnetic behavior of exchange-coupled RE/TM multilayers: low-field spin-flop and magnetoresistance".

12:00 noon R.E. Camley, "Spin configurations in rare-earth, rare-earth/transition metal and other magnetic superlattices".

12:45 pm D. Rokhsar, "Simple theory of exchange coupling in transition metal magnetic multilayers".

1:30 pm B. Heinrich, "Growth and Quantitative Studies of the Exchange Coupling in [Fe(001) whisker]/Cr(001)/Fe(001) Structures."

2:00 pm End of Seminar

Note: Talks will be 30 minute presentations with an additional 15 minutes for discussion.

**Structural properties and  
characterization of multilayered structures**

# ADVANCEMENT IN SOFT MAGNETIC MATERIALS BY MEANS OF MULTILAYERING

H. Fujimori, N. Hasegawa\* and N. Kataoka  
Institute for Materials Research, Tohoku University  
Sendai 980, Japan (\*on leave from Alps Electric Co., Ltd.)

Multilayering of ferromagnetic metals/various kind interlayers can be applied to improve soft magnetic properties in the region of high frequency. The recent development of this method has brought successful advancement in practical materials such as magnetic thin film heads for high density recording and micro inductors for high frequency devices, for examples.

In the Seminar, we will discuss some basic subjects dealing with these soft magnetic multilayered thin films, and present our recent results on Fe/Fe-Hf-C sputtering multilayers with high magnetic permeability (several 1,000) at high frequencies (1 - 100 MHz), high saturation magnetic induction (about 2 T) and high thermal stability (stable even on about 700°C heating).

## 1) Soft magnetism of multilayered thin films

The discussions concerned include following subjects:

Eddy current or skin depth. At high frequencies 1 - 100 MHz, the skin depth of film surface, into which ac-magnetic field can be effectively penetrated, is in the order of magnitude of  $10,000 - 100 \text{ \AA}$  for a metallic magnetic film with permeability 1,000 - 10,000 and specific electrical resistibility  $10 - 100 \text{ \mu}\Omega\text{-cm}$ . Thus, when the thickness of the films practically used (0.1 - 10  $\mu\text{m}$  for most cases) is thicker than the estimated skin depth, multilayering of magnetic and insulating layers is a good method in obtaining high permeability value. (ref. 1)

Domain wall coupling between layers. In thin films, Néel wall can be stabilized rather than Bloch wall. In multilayered films, the energy of Néel wall can further be decreased due to the coupling between Néel and Néel walls in the

near neighbor layers. Such a coupled Néel wall is called the Néel–Néel wall. Therefore, if the wall is pinned at surface roughness or inclusions and the wall coercivity  $H_c$  is related to the film thickness  $D$  as

$$H_c = 1/2M_sD[d\sigma(x)\cdot D(x)/dx],$$

where  $M_s$  is the saturation magnetization,  $\sigma(x)$  the wall energy and  $x$  the coordinates to the wall movement,  $H_c$  can be small by layering and decreased with decreasing the interlayer thickness. (Fig.1, refs. 1,2 and 3)

Domain coupling between layers. In multilayered films, the flux leakage at the edge of film plane can be magnetostatically linked from layer to layer so as to eliminate closure domains which are usually formed in a single film. The closure domains increase anomalous eddy current losses during ac magnetization, thus decrease permeability in the single film. On the other hand, the multilayered film in which no closure domains exist can enhance permeability at high frequencies.

Nanocrystalline soft magnets by multilayering. Amorphous materials are magnetically soft because of a lack of anisotropy as well as a highly homogeneous structure. Similarly to this, nanocrystalline magnets consisting of smaller crystallites than domain wall size, in which the crystallites are cohered and magnetically connected to each other through exchange interaction, are expected to be magnetically soft. Recently, this concept was applied to Fe in order to obtain soft magnets with higher saturation magnetization than amorphous Fe–metalloids alloys. There are now known several methods to produce Fe–base nanocrystalline soft magnets. Among those, multilayered nanocrystalline films such as Fe/Ni–Fe and Fe–C/C are of the pioneer work(ref. 4). After then, nanocrystalline FeSiB–NbCu(ref. 5) and Fe–Hf–C(ref. 6), which can be produced from the amorphous state, have been found.

## 2) Fe/Fe–Hf–C soft magnetic multilayers

We have reported that soft magnetic properties of nanocrystalline Fe–Hf–C films can be improved by multilayering with Fe (ref. 7). The achieved high saturation magnetization of 2.0 T as well as the good frequency dependence

of high permeabilities are remarkable (Fig. 2). In addition, it should be noted that the magnetic properties are extremely stable against heating at high temperatures as around 700°C.

Thus, we have investigated on the high stability of [Fe(250Å)/Fe-Hf-C(250Å)]<sub>5</sub> multilayered film in more details. Composition profiles of these films measured by Rutherford back scattering have revealed fairly weak diffusion between Fe and Fe-Hf-C layers even on anneal at 700°C. X-ray and cross-sectional TEM observations have also shown the suppression of grain growth in the perpendicular direction to film plane. Furthermore, plane-view TEM observations have revealed that the in-plane grain size is as small as the layer thickness and maintained even after anneal at 700°C for 1 hour.

It is considered that 1) the weak interdiffusion is attributed to the stable HfC precipitates existing in the Fe-Hf-C layers and in the vicinity of the interlayer surfaces, and 2) the suppression of grain growth is attributed to the pinning of grain boundaries due to HfC particles existing in upper and lower Fe-Hf-C layers.

#### References

- 1) H. Fujimori, H. Morita, M. Yamamoto and J. Zhang: IEEE Trans. on Magn., Magn-22 (1986) 1101.
- 2) H. Clow: Nature, 194 (1962) 1035.
- 3) F. J. Friedlaender and L. F. Silva: J. Appl. Phys., 36 (1965) 946.
- 4) N. Kumasaka, N. Saito, Y. Shiroishi, K. Shiiki, H. Fujiwara and M. Kudo: J. Appl. Phys., 55 (1984) 2238.
- 5) Y. Yoshizawa, S. Oguma and K. Yamauchi: J. Appl. Phys., 64 (1988) 6044.
- 6) N. Hasegawa and M. Saito: IEICE Technical Report (Japan.), MR8912 (1989).
- 7) N. Hasegawa, N. Kataoka and H. Fujimori: J. Appl. Phys., 70 (1991) 6253.

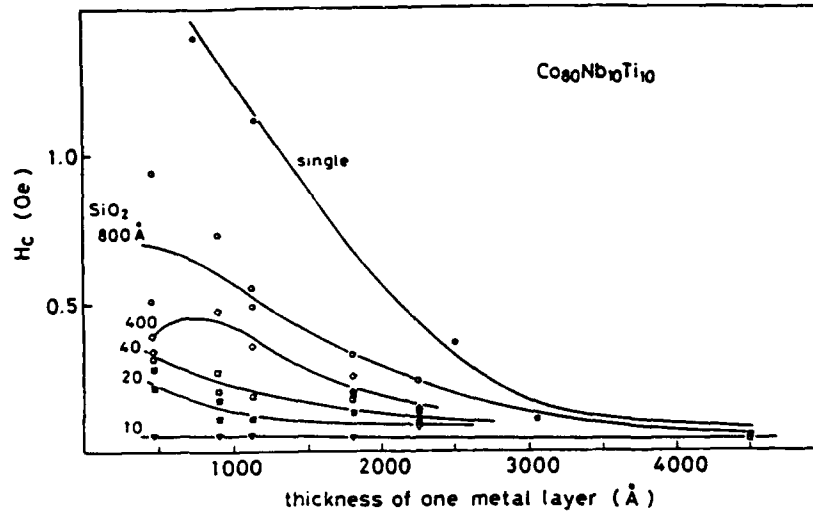


Fig. 1 Coercivity vs. thickness of metal layer for amorphous  $\text{Co}_{80}\text{Nb}_{10}\text{Ti}_{10}/\text{SiO}_2$  multilayered films and  $\text{Co}_{80}\text{Nb}_{10}\text{Ti}_{10}$  films

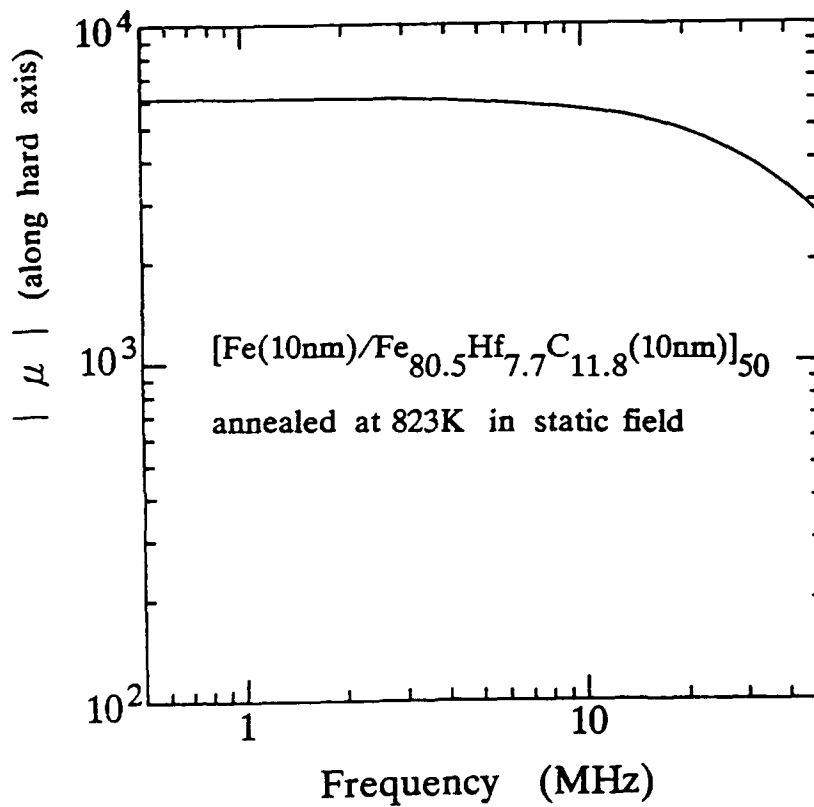


Fig. 2 Magnetic permeability vs. frequency for nanocrystalline Fe/Fe-Hf-C multilayered films

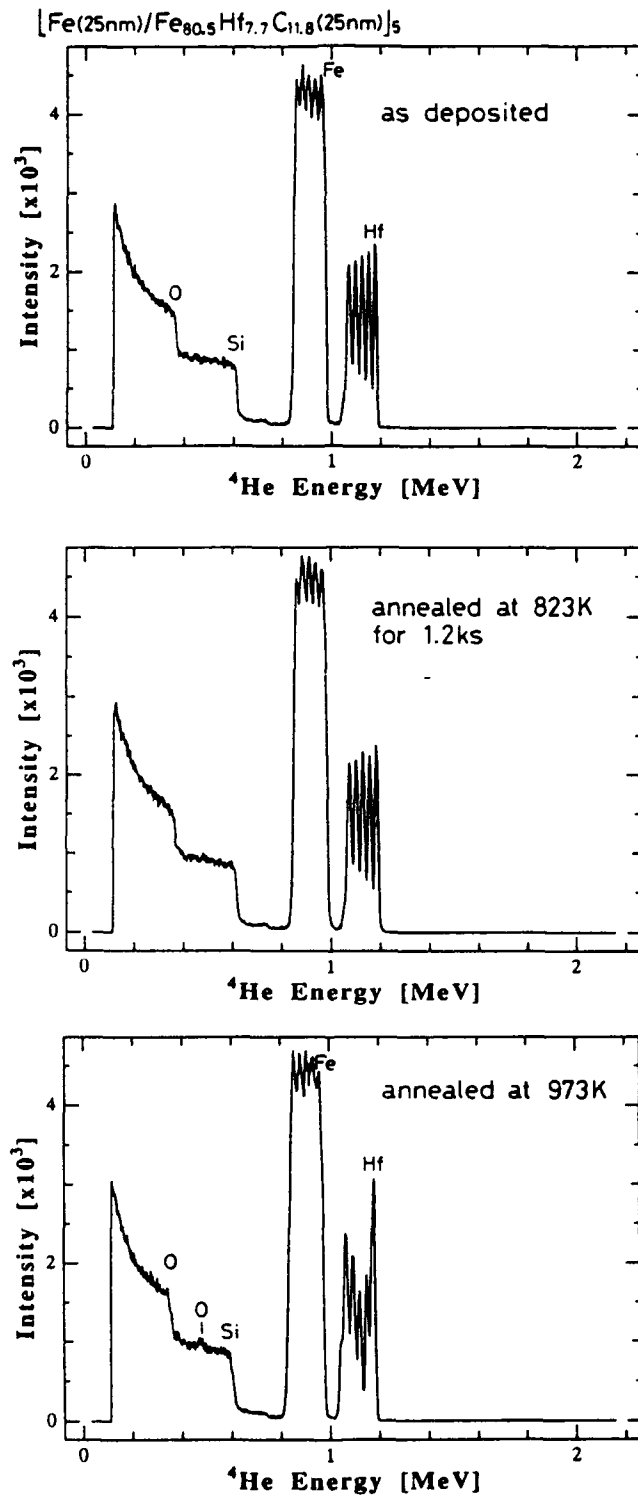


Fig. 3 He-back-scattering profiles for nanocrystalline Fe/Fe-Hf-C multilayered films in the as-deposited and annealed states

"Elastic moduli of metallic multilayered films measured by Brillouin Scattering method"

R. Yamamoto, Institute of Industrial Science, University of Tokyo.

# STRUCTURAL ASPECTS OF SUPERLATTICES UNDER HIGH PRESSURE

Y. Fujii\*

Institute of Materials Science, University of Tsukuba  
Tsukuba, Ibaraki 305, Japan

To study structural aspects associated with its elastic anomaly in a superlattice, we developed a unique x-ray diffraction method on a synchrotron radiation source by using a diamond-anvil high-pressure cell (DAC).<sup>1)</sup> Figure 1 displays its schematic diagram installed at Photon Factory (2.5GeV/350mA, e<sup>+</sup>). By applying hydrostatic pressure accessible to 10GPa to a superlattice specimen, we obtain its linear/bulk compressibility from the Bragg peak shift and analyze its structure from the Bragg intensities. By using this technique, we have studied elastic properties of two metallic superlattices Au/Ni(fcc/fcc)<sup>2)</sup> and Mo/Ni(bcc/fcc)<sup>3)</sup> as well as a semiconductive one PbSe/SnSe<sup>4)</sup>. Figure 2 shows the pressure dependence of lattice-spacings of both the Au(111) buffer layer and the averaged Au/Ni(111) layer measured along the layer-stacking direction of [Au(10A)/Ni(10A)]<sub>50</sub>/Au(250A). The slope of the line drawn in the figure represents compressibility (inverse of elastic modulus) of each layer. The buffer layer shows its compressibility nearly equal to its bulk value while the superlattice is found to be anomalously hard (supermodulus effect?). A similar effect was also found in another metallic superlattice [Mo(20A)/Ni(20A)]<sub>80</sub> in which an anomalous lattice expansion of the Mo(110) layer was observed. In the semiconductive superlattice of epitaxially-grown [PbSe(40A)/SnSe(40A)]<sub>25</sub>, on the other hand, no such anomalous behavior was observed in its compression as shown in Fig. 3. In this case, however, an interesting cubic-to-orthorhombic structural phase transition takes place systematically layer by layer depending upon the layer thickness.

\* Present address: Institute for Solid State Physics, The University of Tokyo, 7-22-1 Roppongi, Minato-ku, Tokyo 106, Japan.

- 1) Y. Ohishi: PhD. Thesis (University of Tsukuba, 1991).
- 2) H. Konishi, Y. Fujii, N. Hamaya, H. Kawada, Y. Ohishi, N. Nakayama, L. Wu, H. Donomae, T. Shinjo, and T. Matsushita: Rev. Sci. Instrum. 63(1), 1992.
- 3) Y. Ohishi, Y. Fujii, N. Nakayama, T. Shinjo, T. Matsushita, and J. Fujita: Multilayers, MRS Intn'l Meeting on Advanced Materials 10, 569 (1989).

4) Y. Ohishi, N. Shingaki, Y. Fujii, Z. Hiroi, N. Nakayama, Y. Bando, and T. Shinjo: High Pressure Research 4, 300 (1990).

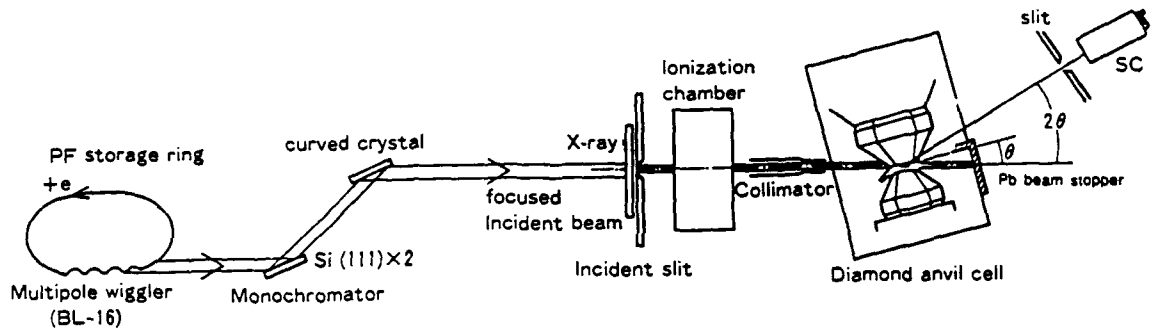


Figure. 1 A schematic drawing of a set-up of the present high-pressure experiments on a multi-pole wiggler beam line at Photon Factory.

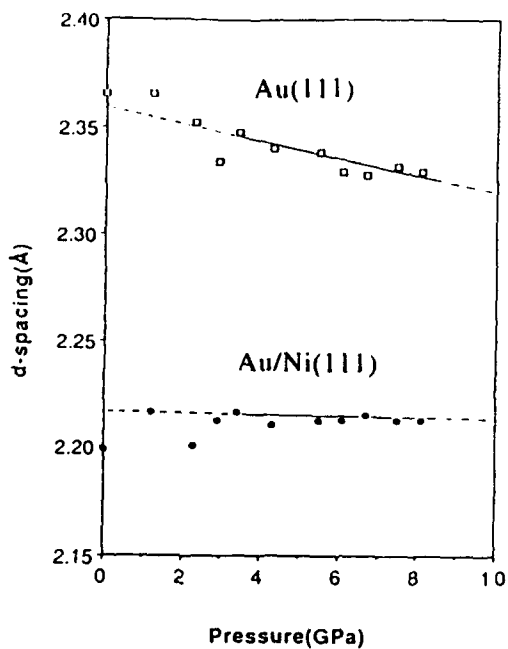


Figure 2.

Pressure dependence of lattice-spacings of Au(111) of the buffer layer and the average (111) of the superlattice. One can see that the superlattice is much less compressible than the buffer layer.

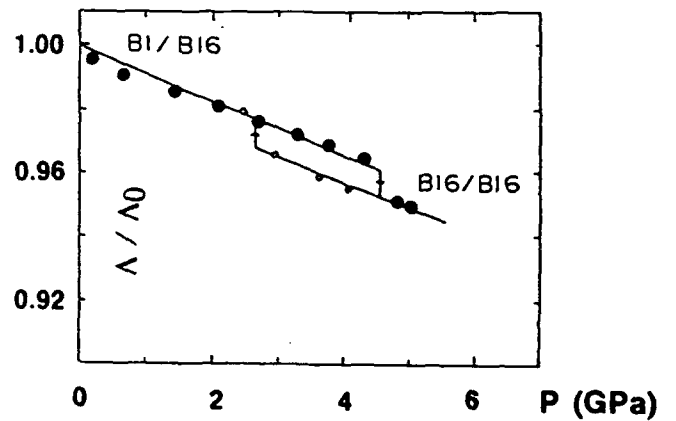


Figure 3.

Linear compression measured on  $[\text{PbSe}(40\text{\AA})/\text{SnSe}(40\text{\AA})]_{25}$ . Closed and open circles represent data points measured in the process of increasing and decreasing pressure, respectively. A large hysteresis is observed.

## Structural Influence on the Magnetic Anisotropy of Co/Pd Superlattices

Charles M. Falco and Brad N. Engel  
Department of Physics and the Optical Sciences Center  
University of Arizona  
Tucson, Arizona 85721

Current interest in the application of Co/Pd and Co/Pt multilayer thin films as media for magneto-optical data storage has been motivated by their strong perpendicular magnetic anisotropy, favorable wavelength dependence, and resistance to corrosion. Although there have been significant efforts to characterize and improve the recording performance of these new media, the underlying fundamental mechanism responsible for perpendicular magnetic anisotropy in metallic multilayers remains unexplained. This is due, in part, to the large variety of thin-film deposition methods and growth conditions commonly used in multilayer fabrication. In order to address this problem, we have created very-well controlled and characterized multilayer films using Molecular Beam Epitaxy (MBE).

We grew a number of single-crystal Co/Pd superlattices by MBE, oriented along the three high-symmetry crystal axes: [001], [110], and [111]. Identical deposition conditions (substrate temperature, evaporation rate, and background pressure) were maintained for all samples to minimize differences in interface diffusion and impurity levels. The structural properties of these multilayers were determined by low and high energy electron diffraction (LEED and RHEED), low and high-angle x-ray diffraction, ion-beam channeling, and Scanning Tunneling Microscopy (STM). We performed a systematic study of the uniaxial magnetic anisotropy in these superlattices, allowing us to determine the structural influences on the interface and bulk contributions to the anisotropy.

We find the dependence of the uniaxial magnetic anisotropy energy on the Co layer thickness in these superlattices to show significant systematic differences for each of the three crystal orientations. Our measurements demonstrate that these variations result solely from differences in the volume contribution to the anisotropy. Our work establishes that the perpendicular interface anisotropy is *independent* of the epitaxial orientation.

Of particular interest are the (001) oriented superlattices. The uniaxial magnetic anisotropy in these films displayed *both* a large perpendicular interface contribution and a large in-plane volume contribution. This competition leads to a crossover from perpendicular to in-plane behavior at  $t_{\text{Co}} = 3 \text{ \AA}$ . Using off-axial x-ray diffraction techniques<sup>†</sup> to measure the fcc (113) Bragg reflection, the in-plane lattice spacing of three samples (one with  $t_{\text{Co}} = 3.7$  and two with  $t_{\text{Co}} = 6.5 \text{ \AA}$ ) is directly measured. These measurements are consistent with a coherent strain model with the Co layers expanded in-plane by  $(8.0 \pm 0.5)\%$  over that of bulk fcc Co. *In situ* RHEED measurements confirm this coherently strained growth for this orientation. An estimate of the in-plane magnetoelastic energy calculated from this strain is in very good agreement with our observed volume anisotropy in these superlattices. This simultaneous existence of the perpendicular interface anisotropy with the in-plane magnetoelastic anisotropy casts doubt on the role of lattice strain in the mechanism of interface anisotropy in Co/Pd.

† In collaboration with L. Wu, N. Nakayama and T. Shinjo, Kyoto University

This work was supported by the University of Arizona Optical Data Storage Center and the U.S. Department of Energy Grant No. DE-FG02-87ER45297.

## Low Dimensional Magnetic and Structural Effects in Single Crystals

### Grown by Molecular Beam Epitaxy

C P Flynn, University of Illinois, Urbana.

New results in two areas of low-dimensional properties are described in this contribution. The first area concerns the modifications of bulk structural order induced by the surface perturbation. In the second area the paper summarizes new results pertaining to several fundamental aspects of the magnetic behavior of single crystal thin epitaxial films and superlattices of magnetic rare earth metals.

It has been predicted for some years that order-disorder phase transformations of the bulk, when viewed in the surface layer alone, may take the appearance of a second order transition. This happens in the theory because a surface skin of disorder, associated with the reduced ordering energy at the surface, spreads into the bulk to a depth that diverges as the bulk transition temperature is approached. Dr J C A Huang and Dr J A Dura, working in my research group, have observed by RHEED, in the growth chamber, the order-disorder transition of  $\text{Cu}_3\text{Au}$  freshly grown by MBE. It was possible to verify experimentally that the RHEED superlattice lines due to the ordering arose 95% from the outer layer alone. Both the (111) and (110) surfaces were observed to exhibit second order structural transitions at temperatures indistinguishable from that of the bulk first order transformation. The measured power law exponents of  $0.57 \pm 0.05$  and  $0.52 \pm 0.02$  in the two cases agree with the mean field value of 0.5.

Our researches in collaboration with Prof. M B Salamon's group and researchers at NIST establish that epitaxial single crystals of rare earths act much like bulk material but with a magnetic phase diagram modified by epitaxial strain and clamping. Non magnetic spacers in superlattices couple successive magnetic layers by a magnetic response similar to that they exhibit in the bulk. Er and Dy, for example, when compressed on Y substrates or spacers, have their bulk ferromagnetism almost completely suppressed; when expanded on Lu, in contrast, the Dy ferromagnetic phase exists almost up to the bulk Néel temperature. The magnetic responses of Y spacers permit coherent coupling of successive magnetic layers up to 150 Å apart along the c axis, but fail to couple over 20 Å along in-plane directions, accurately reflecting Fermi surface symmetry in the RKKY interaction.

Dr F Tsui finds that c axis monolayer alloys of Gd with Y, dominated by in-plane couplings, exhibit remarkable spin glass behavior with critical exponents that correspond to no known universality class.

# **Polarized Neutron Reflection and Diffraction from Magnetic Superlattices**

**Yasuo Endoh**

Department of Physics, Tohoku University  
Aramaki Aoba, Aoba-ku, Sendai, 980 Japan

The interaction between the magnetic moment of neutron and that of the atom depends not only on the magnitudes of the moments but on their orientations relative to one another and the scattering vector  $Q$ . By using polarized neutrons, even complicated microscopic magnetic structures are determined without any ambiguity in principle [1]. Only disadvantage in this method is the weak intensity of polarized neutrons due to the fact that the extraction of polarized neutrons is not ideal at the moment.

Although our early neutron diffraction studies [2] on the magnetism in the multilayers are rarely referred, capability as well as uniqueness of polarized neutron diffraction were demonstrated in the experiments. Then another method of polarized neutron reflection [3] was proposed by G. Felcher which facilitates the study of magnetism in multilayered materials. Now diffraction and reflection experiments using not only neutrons but X-ray are well recognized to be best tools for the study of the multilayers [4,5].

During past few years the multilayer synthesis has been developed quite substantially and then various superlattice films of single crystal are available for the diffraction experiments. In particular the molecular beam epitaxial (MBE) growth is successful in achieving the structural perfection required to unambiguous results of polarized neutron diffraction experiments. A first example is Gd-Y superlattice which was then studied in great detail to show the magnetic structure is

basically determined by the RKKY interaction and the anisotropy induced by the strain in the film [6].

In recent years the new subject of the giant magneto resistance is very attractive due to the fact that the microscopic mechanism is still very puzzling. We have been elucidating this subject by using Fe/Cr multilayered samples synthesized either by electron beam deposition method or MBE method. We present recent neutron diffraction and reflection data and discuss the microscopic mechanism of the giant magneto resistance in Fe/Cr multilayers [7].

The work is supported by the Grant in Aid for the Scientific Research sponsored by the Ministry of Education, Science and Culture.

#### References

- [1] R.M.Moon, T.Riste, W.C.Koehler, Phys.Rev. **181**, 920 (1969)
- [2] M.Sato, K.Abe, Y.Endoh, J.Hayter, J.Phys.C **13**,3563 (1980)
- [3] G.P.Felcher, Phys.Rev. **B24**, 1595 (1981)
- [4] Y.Endoh, C.F.Majkrzak, in Metallic Superlattices ed. by T.Shinjo and T.Takada, ( Tokyo: Elsevier) 1987
- [5] C.F.Majkrzak, J.Kwo, M.Hong, Y.Yefet, D.Gibbs, C.L.Chien, J.Bohr, Adv. Phys. **40**, 99 (1991)
- [6] D.B.McWhan, in The Structure of multilayers ed. by Dhez ( New York: Plenum ) 1988
- [7] N.Hosoito, K.Mibu, S.Araki, T.Shinjo, S.Itoh, Y.Endoh, J.Phys. Soc.Jpn., **61**, 300 (1992)

## **Nuclear Magnetic Resonance Studies of Magnetic Multilayers.**

H. Yasuoka, A. Goto, H. Yamamoto\*, T. Shinjo\*, K. Takanashi\*\* and H. Fujimori\*\*

*Institute for Solid State Physics, University of Tokyo, Roppongi, Tokyo*

*\*Institute for Chemical Research, Kyoto University, Uji-shi, Kyoto*

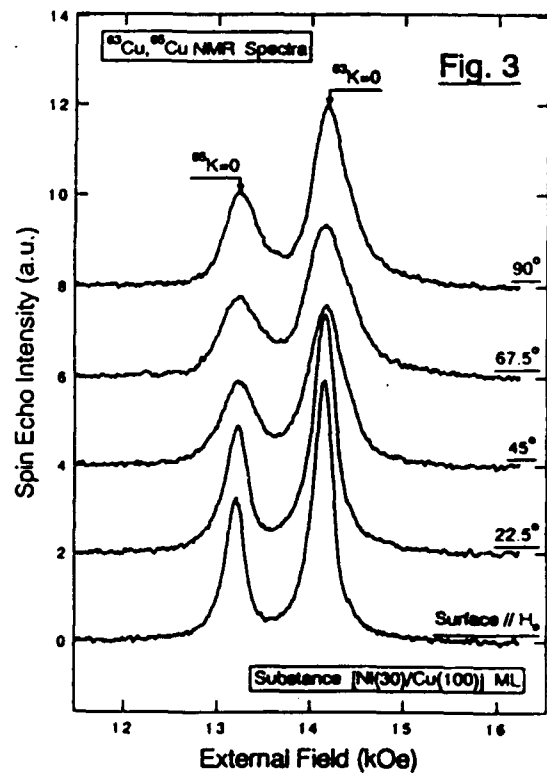
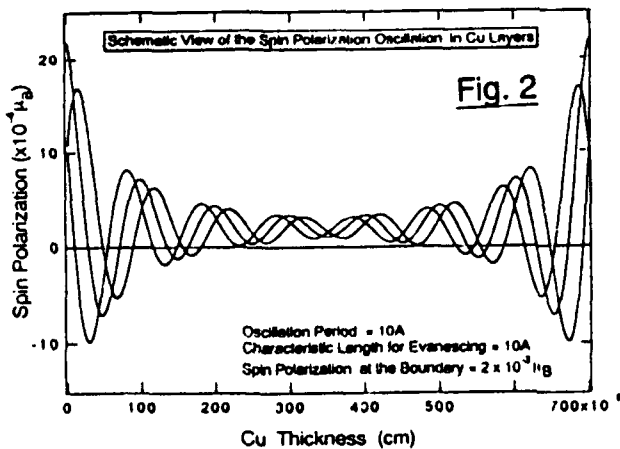
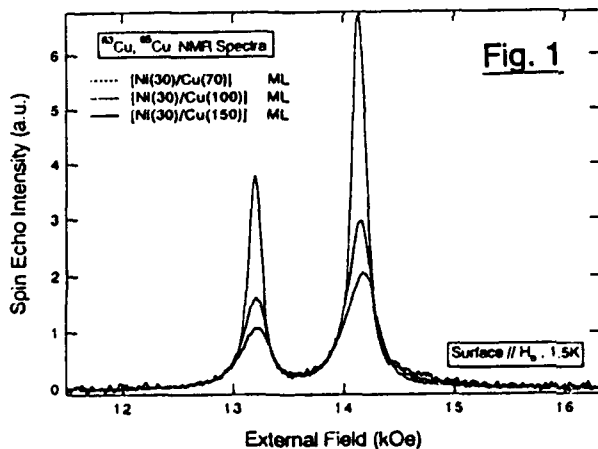
*\*\*Institute for Materials Research, Tohoku University, Katahira, Sendai*

### Abstract

In connection with the giant magnetoresistance and the long range exchange coupling between magnetic layers, the spatial distribution of the local magnetic field in nonmagnetic metallic layers has been investigated using the Nuclear Magnetic Resonance (NMR) technique in [Ni/Cu/Ni] and [Co/Cu/Co] multilayers. From the analysis of the Cu NMR spectra, following two characteristic features have been emerged: 1) The conduction electron polarization in the Cu spacer layers due to the magnetic layers has a long range nature and manifests itself in an oscillatory distribution of the Cu Knight shift, 2) The distribution of the Knight shift, hence the distribution of the magnetic-moment-induced spin polarization in the Cu layers, depends strongly on the orientation of the external magnetic field to the layer plane.

One of the major problems in the system of magnetic multilayered structures is to understand the electronic properties of individual magnetic and non-magnetic layers, as well as the characterization of the structural perfection including the topology of the interface, the lattice coherency, strain etc.. In the case of NMR studies of this respect, the electronic states, or more specifically the distribution of magnetic moments, should be clarified at each atomic layer. Particularly, it is of great importance to understand how the electronic state varies from layer to layer across the interface and how the atomic configuration is modified near the interface where some degree of interdiffusion may occur between the magnetic and nonmagnetic atoms. These features can, in principle, be studied with NMR, because the observed quantities from NMR depend directly on the local electronic states [1]. For such NMR studies, the practical way to perform the experiment and to analyze the data depends on whether we are dealing with atoms in magnetically ordered layers or not. When the nuclei are situated in magnetically ordered state, NMR can be observed at zero field and we obtain the spectrum by changing the frequency for resonance ( this is called specially as Ferromagnetic Nuclear Resonance: FNR ). From the analysis of the inhomogeneously structured FNR spectrum, the atomic topology of the interface has been deduced for several cases [2,3,4]. On the other hand, when the nuclei are situated in the nonmagnetic or nearly magnetic sites, the NMR spectrum is obtained by sweeping the external field at a constant frequency and the shift for resonance (Knight shift) becomes an important physical quantity.

For the study of the interlayer coupling and the anomalous magnetoresistance in magnetic multilayers, it should be quite important to understand how the magnetic spin polarization due to the magnetic layer proceeds into the nonmagnetic spacer layers. This can be demonstrated by the NMR spectrum for the nonmagnetic atoms, in our case Cu atoms, because the distribution of the spectrum correspond directly to the distribution of the local field induced by the magnetic layer via the conduction electron polarization in the spacer layers. Such examples are shown in Fig. 1, where the NMR spin-echo spectra taken at 1.5 K and 16.0 MHz are shown for  $[\text{Ni}(30)/\text{Cu}(x)/\text{Ni}(30)]$  ( $x=70,30,150$  A) multilayers. The spectrum is composed of  $^{63}\text{Cu}$  and  $^{65}\text{Cu}$  nuclei with different nuclear gyromagnetic ratios and the relative intensities of two to one. The Knight shift for the center of the each spectrum is the same as that for the bulk Cu metal, showing that the central part of the spectrum is due to the interior region of the Cu spacer where the magnetic disturbance is less pronounced, and the region decreases with decreasing the Cu thickness. The magnetic disturbance near the interface, we now call this as "the magnetic proximity effect", is most pronounced at the tail of the spectrum. Using a model function for the oscillating conduction electron spin polarization shown in Fig. 2, the shape of the tail can be reproduced with relatively large value of the oscillation period and



characteristic length of damping compared with the conventional RKKY type conduction electron polarization. As is clearly seen in the spectrum, the proximity effect in the [Ni/Cu/Ni] system does not depend on the Cu thickness with the range of 70–150Å. Another remarkable feature was found in the orientation dependence of the spectrum with respect to the layer plane. An example of such data observed in the [Ni(30)/Cu(100)/Ni(30)] is shown in Fig. 3. When the external field, hence the direction of the Ni moment, rotates away from the plane, the distribution of the Knight shift at the tail becomes more negative. That is to say, the local field due to the conduction electron polarization becomes more negative (antiparallel to the external field) as the Ni moments rotate from the plane. The same kind of behavior has also been observed in V resonance shifts in [Fe/V/Fe] and Cu shifts in [Nb/Cu/Nb] superlattices [1,5]. Although the physical origin of this anisotropic nature of the conduction electron polarization, which has not been observed in bulk materials, is not clear at moment, it may be very special to magnetic superlattice.

#### References

- [1] H. Yasuoka: *Metallic Superlattices*, edited by T. Shinjo and T. Takada (Elsevier, Amsterdam, 1987) Chap. 5.
- [2] K. Takanashi, H. Yasuoka, K. Kawaguchi, N. Hosoi and T. Shinjo: *J. Phys. Soc. Jpn.*, 53 (1989) 4315
- [3] K. Le Dang, P. Veillet, Hui He, F. J. Lamelas, C. H. Lee and Roy Clarke: *Phys. Rev.*, 41 (1990) 12904
- [4] H. A. M. de Gronckel, K. Kopinga, W. J. M. de Jonge, P. Panissod, J. P. Schille and F. J. A. de Broeder: *Phys. Rev.*, 44 (1991) 9100
- [5] M. Yudokowsky, W. P. Halperin and Iva K. Schuller: *Phys. Rev.*, B31 (1985) 1673

# Thin film growth on the substrate excited by SAW and in-situ SAW propagation property

Migaku Takahashi, T. Shimatsu, M. Uemura, K. Sagara, S. Sakakibara  
Dept. of Electronic Engng. Tohoku Univ.  
Aoba, Aramaki, Aoba-ku, Sendai 980

## Abstract

The mechanism of film growth onto  $\text{LiNbO}_3$  substrate excited by SAW (Surface Acoustic Wave) was discussed. In-situ measurement of propagation of SAW was made during film deposition, and also the topology of film surface was observed by STM for evaporated and sputtered Fe films, respectively. From the measurement of propagation properties, the appearance of minimum of normalized output  $V/V_{\text{initial}}$  against film thickness was found for all film examined. The film thickness where  $V/V_{\text{initial}}$  takes minimum corresponds to the critical thickness where the film structure changes from island to continuous structure. This critical film thickness in evaporated Fe ( $\approx 30\text{\AA}$ ) was found to be different from that of sputtered Fe ( $\approx 20\text{\AA}$ ). Compared to these critical film thickness ( $\approx 30\text{\AA}$ ) with that of non-excited one ( $\approx 60\text{\AA}$ ), the initial film growth is strongly influenced by the application SAW excitation.

## 1. Introduction

Authors have already reported that microstructure and morphology of the Mo-permalloy and Co-Cr-Ta films fabricated onto the substrate excited by SAW were found to be drastically changed<sup>1-3)</sup>. In the

present study, in order to make clear the effect of SAW to initial film growth, the in-situ propagation properties of SAW excitation were investigated during deposition of metal films. Based on these results, the relation between the propagation properties of SAW and initial growth of the films is discussed in connection with the film topology determined by STM.

## 2. Experimental Procedure

Fig.1 shows the schematic view of the substrate used in this experiment.  $128^\circ$  rotated Y-cut  $\text{LiNbO}_3$  single crystal was used as the piezoelectric substrate. SAW was propagated along X-axis in this plane. SAW at a frequency of 45MHz was excited by the interdigital transducer (IDT). The change of a normal SAW amplitude component  $U_{0-p}$  and in plane SAW amplitude

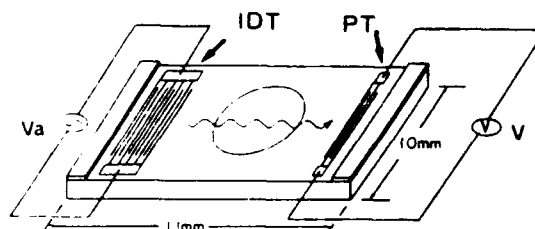


Fig.1 The schematic view of  $\text{LiNbO}_3$  single crystal substrate. The opposite side surface is rough to eliminate bulk waves. Absorbers are deposited on both sides of the substrate in order to avoid the reflections of SAW.

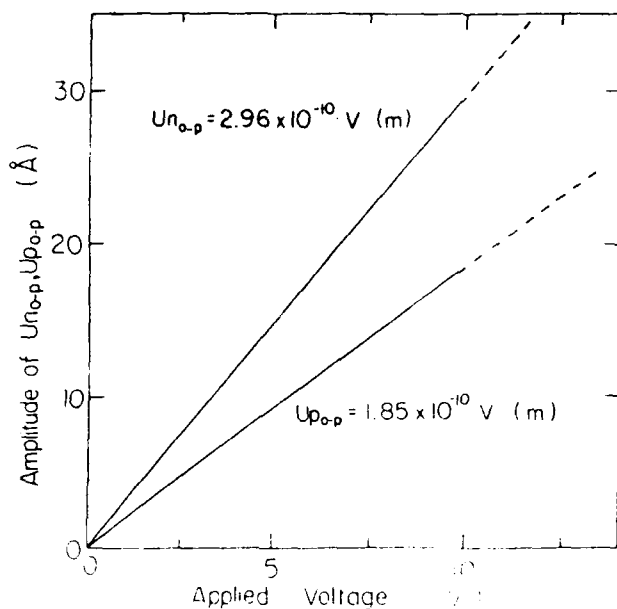


Fig.2 Relationship between applied voltage to IDT and excitation amplitude.

component  $U_{p-o-p}$  are shown in Fig.2 against applied voltage to IDT. The passive transducer (PT) is attached 6.5mm further from IDT. Propagation properties of SAW were determined by measuring the voltage ratio  $V/V_{initial}$  using Lock-in amplifier.  $V$  corresponds to output voltage at PT during deposition and  $V_{initial}$  corresponds to initial voltage at PT before deposition. Fe films up to 300Å were deposited by electron-beam and also d.c. magnetron sputtering, respectively. Film diameter is 5mm $\phi$ , which size is smaller than the propagation width of SAW (6mm).

### 3. Results

Fig.3 shows the change of output voltage as a function of deposition time during Fe evaporation (deposition rate is varied from 0.5 to 5A/s) with SAW excitation, respectively. Vertical axis,  $V/V_{initial}$ , is the normalized

ratio of output voltage at PT. Horizontal axis corresponds to equivalent total film thickness calculated from the deposition rate and deposition time. In the case of deposition rate 5A/s and applied voltage 5V,  $V/V_{initial}$  doesn't change up to 10Å and then with slight increase of film thickness suddenly decreases and exhibits minimum about 0.1 at the film thickness of about 30Å. With further increasing film thickness more than 30Å,  $V/V_{initial}$  again increases and becomes constant about 0.3. Similar change of  $V/V_{initial}$  against film thickness is obtained in the case of Fe films fabricated at excited voltages 3 to 8V and deposition rates 0.5 to 5A/s, as seen in this figure.

Fig.4 shows two kinds of the STM images of the top surface of evaporated Fe films with the thickness of 300Å. One is prepared at deposition rate 5A/s without SAW excitation and the other with SAW excitation at 7V. In the film at applied voltage 7V, a remarkably smooth surface compared to the non-excited one was realized.

Fig.5 shows the propagation property in sputtered Fe film (deposition rate 5A/s) at applied voltage 3V. In the same figure, the propagation property in evaporated Fe film fabricated under the same deposition rate and applied voltage was also shown for comparison. The propagation property of sputtered Fe film shows a similar behavior observed in the case of evaporated Fe films. However, the film thickness where  $V/V_{initial}$  takes minimum is about

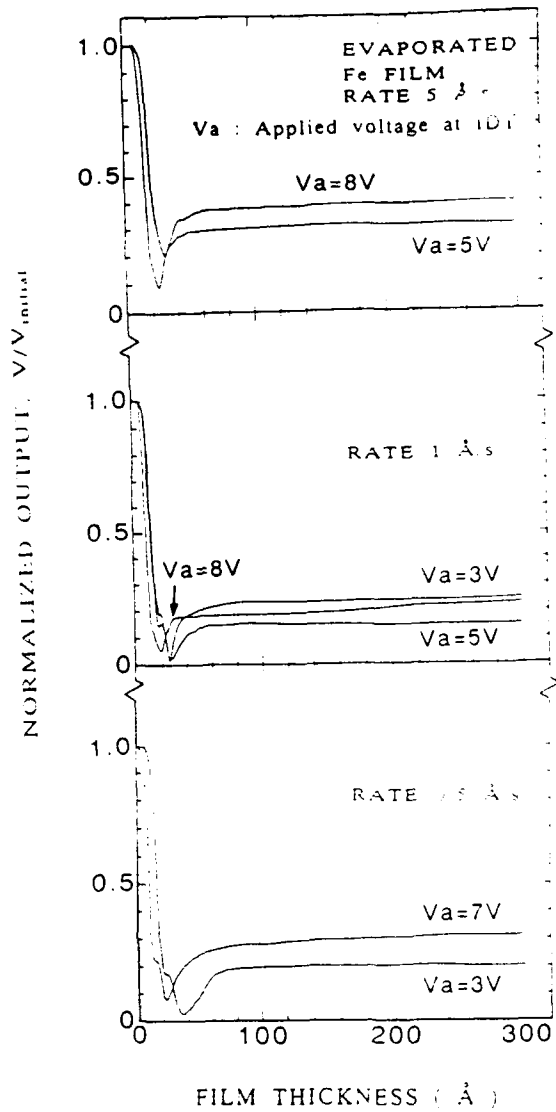


Fig.3 Dependence of normalized output,  $V/V_{initial}$ , on film thickness calculated from the deposition rate and deposition time during Fe evaporation with SAW excitation. Deposition rate is varied  $5 \sim 0.5 \text{ \AA/s}$ .

20A for sputtering. This critical film thickness is smaller than the value of 30A obtained for evaporated Fe film.

In order to make clear the effect of SAW excitation on film growth more precisely, three kinds of experiment are further carried out in the case of evaporated Fe film. In this case, deposition rate is fixed at  $1 \text{ \AA/s}$  and applied voltage is fixed at 3V. Namely, (I)

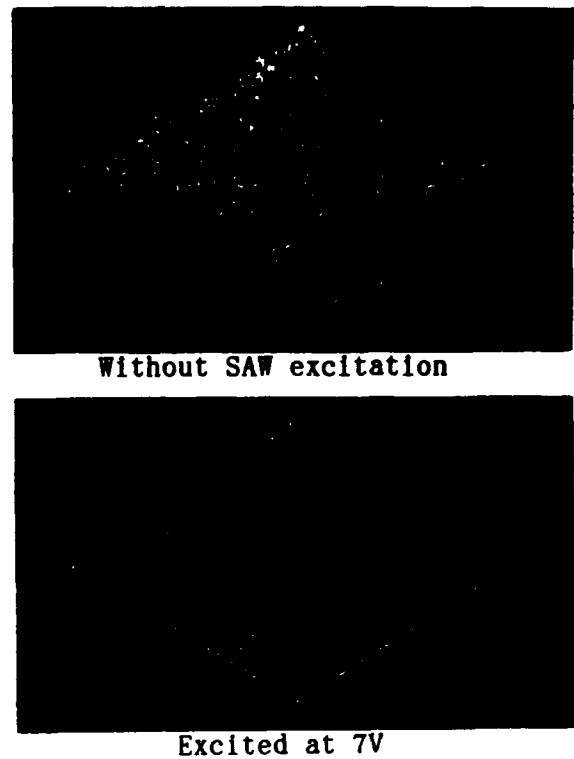


Fig.4 STM images of the top surface of the evaporated Fe films with film thickness of 300A prepared on the substrate without and with SAW excitation at 7V.

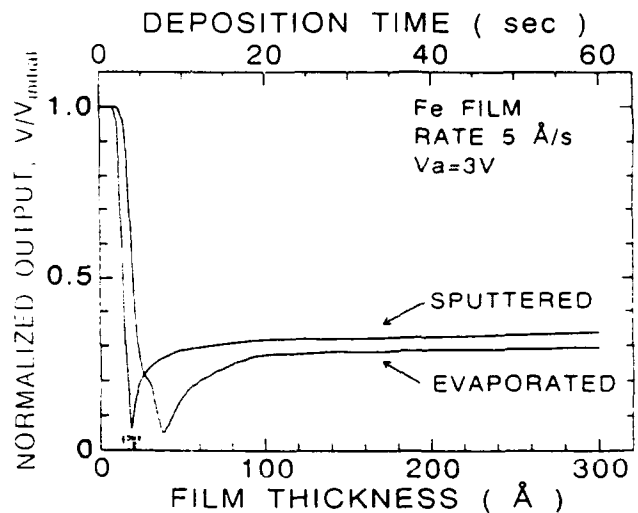


Fig.5 Dependence of normalized output,  $V/V_{initial}$ , on film thickness calculated from the deposition rate and deposition time during Fe sputtering and evaporation with SAW excitation at 3V.

Continuous evaporation; evaporation is made continuously onto the continuously excited substrate by

SAW (continuous mode), (II) Step evaporation; evaporation is made steply onto the continuously excited substrate by SAW (step mode), (III) Non SAW excitation; evaporation is made steply onto the non-excited substrate by SAW.

In each mode, measurement of propagation properties of SAW was made at various fixed film thickness within a same vacuum evaporator. These three different kinds of results are shown in Fig.6. As seen in this figure, the difference of the propagation properties between continuous evaporation (I) and step evaporation (II) was not found. Furthermore, each data point does not change its value as a function of time. Therefore, this fact means that the kinetic structure relaxation of atoms which are once trapped at the substrate surface is not influenced by the presence of SAW on the substrate. However, comparing the propagation properties of continuous (I) and step evaporation (II) with that of non SAW excitation (III), one can easily find that the big difference is caused by the application of SAW. Namely, the critical film thickness at which  $V/V_{initial}$  takes minimum is completely different each other. Namely, in the case of mode (I) and (II), this critical film thickness is about 30Å, however, in the case of mode (III), this film thickness becomes to be about 60Å. Such difference is mainly caused by the change of initial film growth caused by the presence of SAW during deposition. For detailed mechanism of this matter, discussion will be developed in the later section.

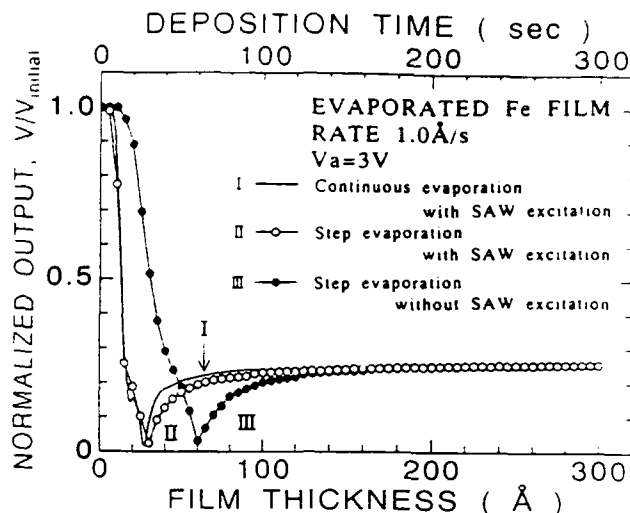


Fig.6 Dependence of normalized output,  $V/V_{initial}$ , on Fe film thickness. Continuous (I) and step (II) evaporation with SAW excitation at 3V and step evaporation without SAW excitation (III).

#### 4. Discussion

##### 4-1. Propagation properties

From the measurement of propagation properties, two unique features are clarified. One is the steady attenuation of  $V/V_{initial}$  at thick film nearly 300Å. And the other is the appearance of minimum of  $V/V_{initial}$  around 30Å in film thickness.

In Fig.7, in order to explain the steady attenuation of  $V/V_{initial}$  observed at the thickness of 300Å, a simple model by taking into account the phase shift of SAW is proposed. Generally, if the conductive metallic film will cover the top surface of the piezoelectric substrate, the propagation velocity of SAW becomes slower compared to that of free surface due to the short of the surface electric field on the substrate. Furthermore, in the case of the circular film, the path length of SAW within the metallic circular film at which SAW

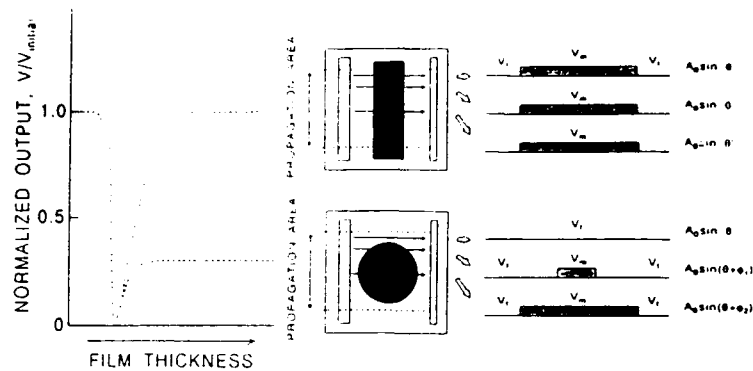


Fig.7 Phase shift of SAW at PT due to the conductive circular film on the piezoelectric substrate.

passes over is different from point to point. Therefore, the coherent phase shift of SAW at thick film nearly 300Å is induced at PT and as a result  $V/V_{initial}$  attenuates.

According to this simple model, it is expected that no attenuation takes place in the case of square conductive film because of no difference in path length of SAW at energy points within the conductive film. In fact, it was confirmed experimentally that no attenuation of  $V/V_{initial}$  was detected in the square shaped evaporated film of Fe at the thickness of 300Å.

Therefore, it is concluded that the attenuation of  $V/V_{initial}$  observed at thick film nearly 300Å is mainly caused by the coherent phase shift of SAW, affecting the difference of the geometrical path length of SAW within the conductive circular film.

Discussion is further developed for the appearance of minimum of  $V/V_{initial}$  observed at nearly 30Å in film thickness. Especially, the film growth at initial stage is discussed in connection with the propagation properties.

In Fig.8, the propagation

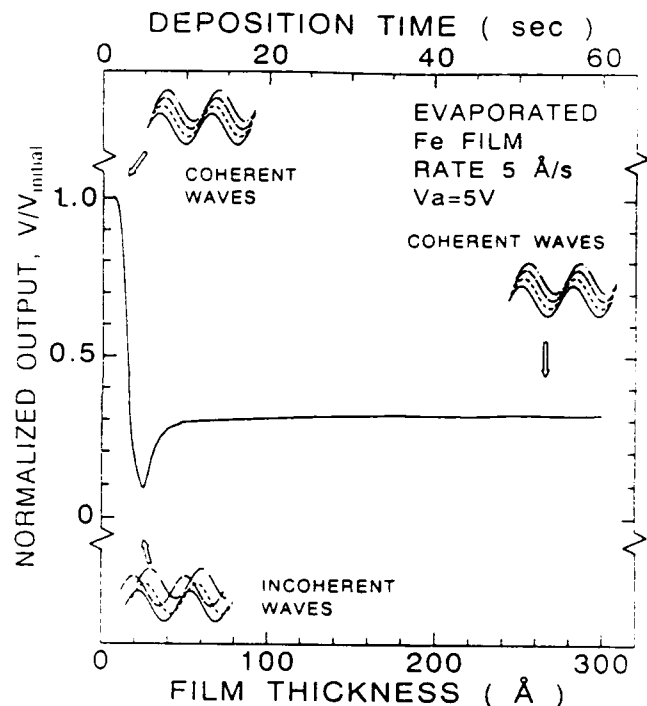


Fig.8 The propagation property of SAW for evaporated Fe film with schematic model of SAW at each film thickness.

property of SAW for evaporated Fe film at each film thickness is shown with schematic model of phase shift of SAW at PT.

At the beginning of film growth, size of nucleus of metallic Fe film which causes short of surface electric field on the substrate is much smaller than the wave length of SAW about 88 $\mu$ m. Therefore, velocity dispersion of

SAW is not took place (i.e. coherency of SAW at PT), and as a result,  $V/V_{initial}$  shows constant value of 1.0 at PT up to several  $\text{\AA}$  in film thickness. With increasing film thickness, nucleus agglomerates together and film structure may change from island to continuous structure. Such morphological change will cause the enhancement of short of surface electric field on the substrate. As a result, the velocity dispersion of SAW increases. Therefore,  $V/V_{initial}$  at PT rapidly decreases because of sudden increment of velocity dispersion of SAW (i.e. incoherency of SAW at PT). With further increasing film thickness,  $V/V_{initial}$  again increases and becomes constant about 0.3 because of coherent phase shift of SAW at PT due to the homogeneous short of surface electric field on the substrate.

According to this simple assumption, it is supposed that the thickness where  $V/V_{initial}$  takes minimum corresponds to the critical thickness at which the film structure changes from island to continuous structure.

#### 4-2. Initial film growth

The effect of SAW excitation to morphology of Fe film was found to be remarkable. Here, based on the results of STM images and propagation properties, the effect of SAW excitation on initial film growth is discussed.

As already stated in previous section 4-1, the critical film thickness at which  $V/V_{initial}$  takes minimum is changed to thinner thickness and the surface roughness

becomes smaller and smaller by the application of SAW, compared to that of non SAW excitation. These experimental facts suggest that the density of nucleus for the films fabricated with SAW excitation becomes higher compared to that of non-excited one by SAW, under the physical conditions that the average film thickness and also the sizes of nucleus remain constant. Namely, concerning for the initial growth, application of SAW changes its growth from islandlike (non SAW excitation) to layer-by-layerlike structure.

Based on this physical assumption, in Fig.9, the schematic models of the film surface at the initial growth of evaporated Fe films without and with SAW excitation are shown respectively. The relative size of nucleus and density of nucleus are estimated from (1) the period of surface roughness in the STM images, by assuming that the surface morphology at film thickness 300 $\text{\AA}$  is determined by simple trace of initial layer and (2) the critical thickness at which  $V/V_{initial}$  at PT takes minimum in SAW propagation property.

As seen in the figure, in the case of evaporated Fe films, the density of nucleus is found to increase by SAW excitation compared to that of the film of non-excited one. However, within the accuracy in this experiment, the precise information for the size of nucleus is now under question.

The effect of SAW excitation on initial film growth for different deposition methods, namely, sputtered and evaporated Fe film is

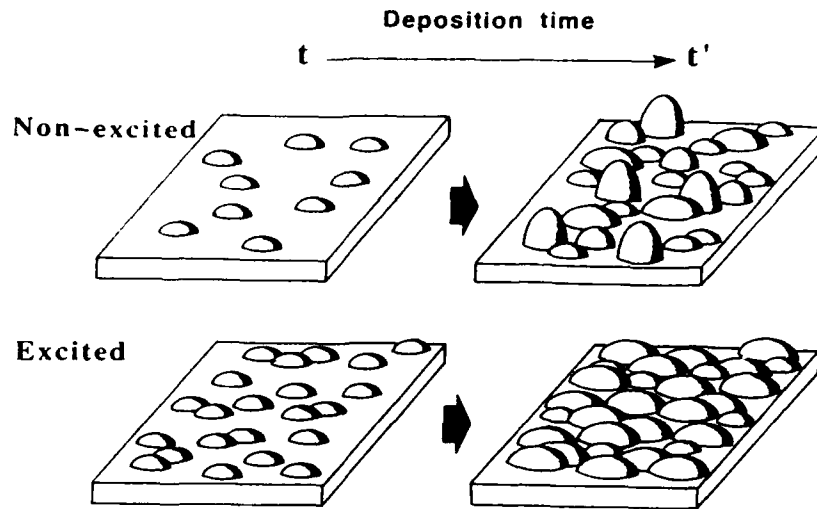


Fig.9 The schematic model of the film surface at the initial growth of evaporated Fe film without and with SAW excitation.

also discussed. In the case of sputtered Fe film, density of nucleus gradually increases with increasing the excitation amplitude. Such change is similar to that of evaporated Fe films. However, from the results of SAW propagation properties, the critical film thickness from island to continuous structure in sputtered Fe film was found to be about 20Å. This critical value in thickness is lower than that of evaporated one ( $\approx 30\text{Å}$ ). The main reason of this difference may be attributable to the difference of the surface mobility on substrate surface, due to the different kinetic energy of atoms sputtered or evaporated.

#### [References]

- 1) Migaku Takahashi, A.Fujita, T.Shimatsu, T.Wakiyama, J.Yamada, T,Shiba : *IEEE Trans.Magn.*, **MAG-26**, 1453 (1990)
- 2) Migaku Takahashi, A.Fujita, T.Shimatsu, T.Wakiyama, J.Yamada, T,Shiba : *J.Magn.Soc.Jpn.*, **14**,323 (1990)
- 3) Migaku Takahashi, A.Fujita, T.Shimatsu, T.Wakiyama, J.Yamada, T,Shiba : *J.Magn.Soc.Jpn.*, **15**,323 (1991)

PHYSICAL PROPERTIES OF MULTILAYERED FCC-Fe/Cu(100)  
AND Fe/Cu(111) ARTIFICIAL LATTICE

S. Mitani\*, K. Doi\*, H. Toyoda\*, M. Matsui\* and M. Doyama\*\*

\* Department of Materials Science and Engineering, Faculty of Engineering  
Nagoya University, Furocho, Chikusa-ku, Nagoya, 464-01 Nagoya Japan

\*\* Department of Materials, The Nishi Tokyo University, Uenohara, Yamanashi  
409-01 Japan

Multilayered Fe/Cu films have been epitaxially grown on a copper single crystal. On Cu(100) surface fcc-Fe / Cu (100) multilayers have been obtained and the magnetic moment was  $2.0 \pm 0.1 \mu_B/\text{Fe}$ . The film [2.8 MLFe/10 MLCu]<sub>30</sub> on Cu(100) shows perpendicular magnetization at 5K. The Curie temperature ( $T_c$ ) of [10MLFe/10Cu]<sub>20</sub> on Cu(100) was 578 K.  $T_c$  decreases with decreasing the number of Fe layers. On Cu (111), Fe layer was grown and it has island-like bcc domain structure. The bcc-Fe films are also ferromagnetic and the magnetic moment is  $2.2 \mu_B/\text{Fe}$ . The Curie temperature is lower than that of bulk bcc Fe.

Multilayered film of [nFe/mCu] ( $n=2.8 \sim 10$   $m=10$ ) were grown epitaxially on Cu(100) and Cu(111). The substrate temperature was about 53°C to 100°C. The RHEED pattern of iron layer epitaxially grown on Cu(100) shown in Fig.1(b) is streak-like and similar to the Cu(100) pattern suggesting that the multilayered iron has fcc structure. The X-ray diffraction reveals the multilayered structure of film as shown in Fig. 2. Figures 3 and 4 show the magnetization curve of the sandwiched and multilayered Fe/Cu(100) films at 5K, respectively. The magnetic easy axis of the films is in plane except for [2.8MLFe/10MLCu]<sub>30</sub> which shows perpendicular anisotropy. Figure 5 shows the magnetization of fcc Fe/Cu films at 10 kOe as a function of total number of Fe layers. The slope corresponds to  $2.0 \pm 0.1 \mu_B/\text{Fe}$ . The maximum number of fcc layers obtainable on Cu(100) was 20ML. The temperature dependence of magnetization was measured and the results are shown in Figs.6 and 7. The Curie temperature ( $T_c$ ) of [10 MLFe/10 Cu]<sub>20</sub> was found to be 578 K and that of [2.8MLFe/10MLCu]<sub>30</sub> about 400 K. The Curie temperature was decreased with the decreasing the number of Fe layers.

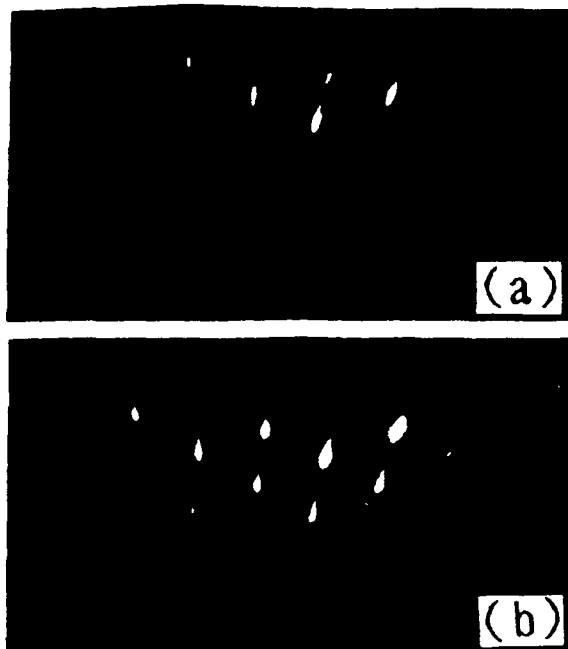


Fig. 1. (a) RHEED pattern taken for the Cu(100) substrates  $[011]$  azimuth, (b) RHEED pattern taken for the  $[2.8 \text{ ML Fe}/10 \text{ ML Cu}]_{30}$  film,  $[011]$  azimuth

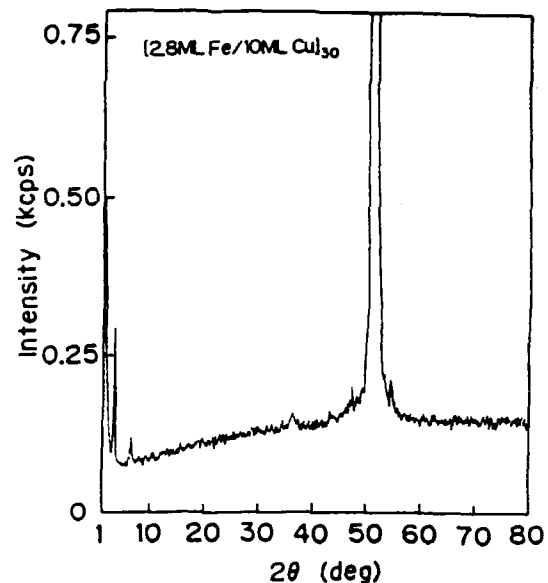


Fig. 2. X-ray diffraction pattern taken for the  $[2.8 \text{ ML Fe}/10 \text{ ML Cu}]_{30}$  film

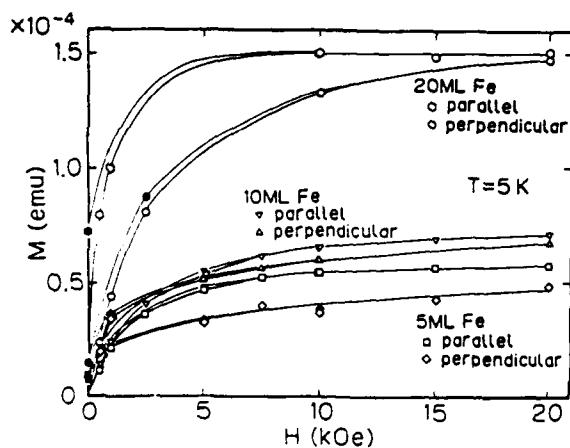


Fig. 3. Magnetization curves of sandwiched films: open symbols with increasing magnetic field, closed symbols with decreasing magnetic field.

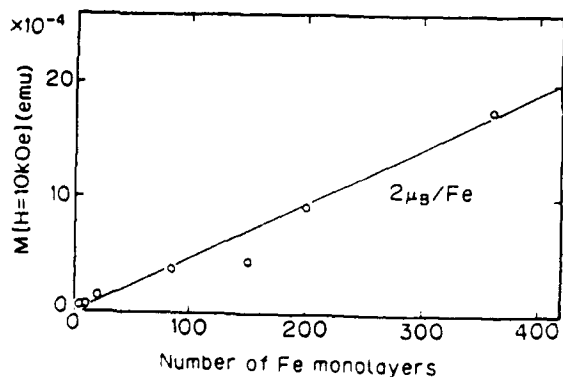


Fig. 5. Magnetization as a function of total number of Fe layers in the film.

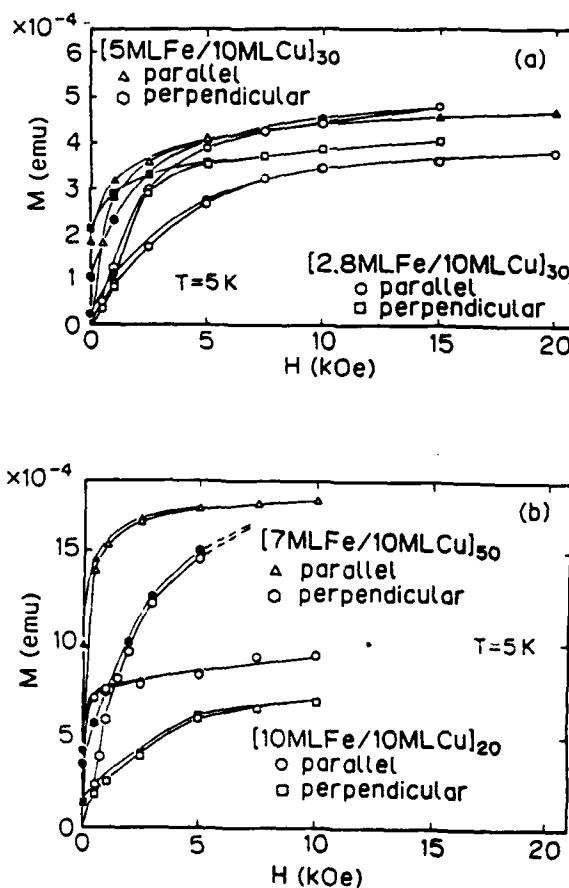


Fig. 4. Magnetization curves of multilayered fcc-Fe/Cu films: open symbols with increasing magnetic field, closed symbols with decreasing magnetic field: (a)  $[2.8 \text{ ML Fe}/10 \text{ ML Cu}]_{30}$  and  $[5 \text{ ML Fe}/10 \text{ ML Cu}]_{30}$ ; (b)  $[7 \text{ ML Fe}/10 \text{ ML Cu}]_{50}$  and  $[10 \text{ ML Fe}/10 \text{ ML Cu}]_{20}$ .

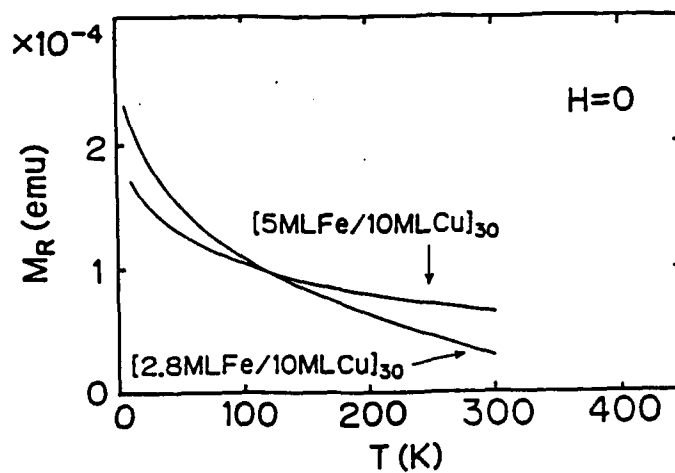


Fig. 6. Residual magnetization for the  $[2.8\text{ML Fe}/10\text{ML Cu}]_{30}$  film and the  $[5\text{ML Fe}/10\text{ML Cu}]_{30}$  film as a function of temperature.

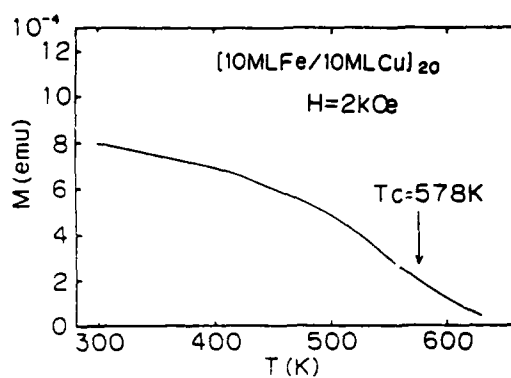


Fig. 7. Magnetization for the  $[10\text{ML Fe}/10\text{ML Cu}]_{20}$  film in the field of 2 kOe as a function of temperature.

# **Magnetoresistance**

## MAGNETIC STRUCTURE AND MAGNETO-TRANSPORT PROPERTIES OF MULTILAYERS WITH TWO MAGNETIC COMPONENTS

Teruya SHINJO

*Institute for Chemical Research, Kyoto University  
Uji, Kyoto-fu 611, Japan*

Magneto-transport phenomena of multilayers with two magnetic components are studied. The samples with the structure of e.g. [Cu/Co/Cu/NiFe] $x_n$ , were prepared by ultrahigh vacuum deposition technique. If the non-magnetic spacing layers are thick enough, each magnetic layer may behave independently. Because the coercive forces of Co and NiFe alloy (permalloy) layers are different, the two magnetizations are oriented antiparallel in a certain field region, during the field sweeping. Then, the resistivity increases remarkably. As far as the magnetizations are oriented antiparallel, the spin-dependent scattering works and a large magnetoresistance (MR) effect occurs, similarly to the well-known giant MR effect observed in Fe/Cr and Co/Cu multilayers. The MR effect of such non-exchange type multilayers is significantly large in a very small field region, which seems to be advantageous for technical applications.

By rotating a small external field, the resistance of multilayer with two magnetic components is measured as a function of angle between two magnetizations. In the case of a sample with 100Å Cu layers, the magnetization of NiFe layer easily follows the change of the external field direction (20 Oe). While, the other (Co layer magnetization) remains in the original field direction. The dependence of the MR effect on the relative angle is found to be well represented by a sinusoidal curve. If the spacing layer thickness is 55Å, on the other hand, the angle dependence deviates from an ideal sinusoidal curve. The line profile is analyzed by assuming an interlayer exchange interaction, and the magnitude of the exchange field acting at the NiFe layer, caused by the adjacent Co layer magnetizations, is estimated to be about 7 Oe. If the Cu layer thickness is less, the exchange interaction becomes stronger and the two magnetic components cannot behave independently. The interlayer exchange interaction was studied by preparing samples with various Cu layer thicknesses. However, the results crucially depend on the

roughness of each layer and quantitatively conclusive results are not yet obtained.

Similar experiments were carried out also for Au- and Ag-based samples where Au or Ag were used as the non-magnetic spacing materials instead of Cu. The effects of buffer layers and surface modifications are examined for Ag-based samples. The flatness of very thin Ag layers is in general worse than the other, Cu or Au cases and accordingly the Ag-based samples prepared without buffer layers do not show a large MR effect. However by using Cr buffer layers, the flatness of Ag layers is improved and a large MR effect is observed. It has been revealed that, among Cu-, Au- and Ag-films, the magnetic properties are very similar and the MR characteristics are not significantly different.

In order to clarify the role of interface, modifications of magnetic layer surface were attempted in the following way. Before and after the deposition of Co layers, a Cr layer with 2A thick was deposited. The nominal structure is, therefore, [Ag/Cr(2A)/Co(25A)/Cr(2A)/Ag/NiFe]. The hysteresis curve suggests that the isolation of two magnetic component is excellent and an antiparallel alignment is well established. However, the observed MR ratio is extremely small. The spin-dependent scattering is thus almost killed by a Cr monolayer at each interface. This result suggests that the spin-dependent scattering mainly occurs at interface sites. On the other hand, by depositing Co monolayers on the interfaces of NiFe layer, the MR ratio is increased and thus it is hoped that MR characteristics are improved by such interface modifications.

Preliminary results from Mossbauer spectroscopic studies will also be introduced. The temperature dependence of the local magnetization at an interface site of NiFe layer is studied from Fe-57 measurements. Au-197 measurements are useful to estimate the spin density distribution in Au layers and also to obtain a unique information on lattice dynamics.

# Giant Magnetoresistance in FeNiCo/Cu Multilayers

Mutsuko Jimbo\*, Tatsuya Kanda, Shigeru Tsunashima,  
Susumu Uchiyama and Tetsuo Kato\*

Dept. Electronics, Nagoya Univ. 464-01 Nagoya, Japan  
\*Mater. Engineering Lab., Daido Inst. of Tech. 457 Nagoya, Japan

**Abstract-** The giant magnetoresistance effect of (FeNiCo/Cu) multilayers prepared by RF magnetron sputtering method is reported. Magnetoresistance ratio as large as 35% is obtained at 300K and it changes oscillatory as a function of Cu layer thickness. The oscillation period is about 1nm, which is similar to the case of (Co/Cu) multilayers. In (FeNiCo/Cu) multilayers, the saturation field decreases rapidly when Cu layer thickness varies slightly around the peak position of the magnetoresistance.

## 1. Introduction

A considerable number of studies have been made on the giant magnetoresistance (GMR) in multilayers since the report of GMR in Fe/Cr multilayers [1]. Further studies have reported the oscillation of magnetoresistance as a function of nonmagnetic layer thickness [2-4]. The GMR effect is attracting great interest for technological applications such as magnetoresistance (MR) magnetic heads and sensors. These MR devices require large MR changes at low magnetic field. Thus several kinds of multilayers with large MR at low field have been developed as follows. In (NiFe/Cu/Co/Cu) multilayers [5], a MR ratio of about 9% at 300K have been reported with a saturation field of 500 Oe which is much smaller than that in (Co/Cu) and (Fe/Cr) multilayers. In (Ta/NiFe/Cu/NiFe/FeMn/Ta) sandwiches [6], MR of 5% have been also obtained at room temperature in 10 Oe.

In this paper, we choose a soft magnetic alloy, FeNiCo, as the magnetic layer, because this alloy can be expected to obtain larger MR than NiFe owing to containing Co atoms, and report on the magnetoresistance in (FeNiCo/Cu) multilayers which varies oscillatory as a function of Cu layer thickness. We show further that the saturation field is more sensitive than the MR ratio Cu layer thickness.

## 2. Experimental

(NiFeCo/Cu) multilayers were prepared by RF magnetron sputtering in an argon pressure of 5mTorr with applying a magnetic field (40 Oe)

in the film plane. The deposition rates of NiFeCo and Cu were about 0.1 nm/s. The samples were deposited on glass substrates with Fe buffer layer (5 nm thick). The composition of FeNiCo is Fe 16at%, Ni 66at% and Co 18at%. In this composition, both the magneto-crystalline anisotropy and magnetostriction constants are known to be approximately zero [7]. Nominal layer thicknesses were determined from the deposition time and the bilayer period was confirmed by low angle X-ray diffraction measurement. The NiFeCo layer thickness was fixed at 1.5nm and the Cu layer thickness was varied between 0.7 and 4nm. The magnetoresistance was measured with the conventional d.c. four probe method on  $2 \times 15 \text{ mm}^2$  samples with a dimension of  $2 \times 15 \text{ mm}^2$ .

## 3. Results and Discussion

Fig.1 shows the dependence of saturation MR ratio  $(R_{\text{max}} - R_{\text{min}}) / R_{\text{min}}$  on Cu layer thickness  $t_{\text{Cu}}$  at room temperature for  $\text{Fe}(5\text{nm}) / [\text{NiFeCo}(1.5\text{nm}) / \text{Cu}(t_{\text{Cu}}, \text{nm})]_N$  multilayers, where N is a number of bilayers. From this figure, two clear peaks and a broad peak are seen at thickness of about 0.8, 2.2 and 3.5nm, respectively. The period of oscillation is about 1nm similar to those in (Co/Cu) [2,3] and most of other multilayers [8]. At the first peak of  $t_{\text{Cu}} = 0.8\text{nm}$ , the maximum MR ratio as large as 35% is obtained for  $N=30$ . While at the second peak ( $t_{\text{Cu}} = 2.2\text{nm}$ ), the maximum value of 13% is obtained for  $N=10$  but not for  $N=30$ . This is thought resulting from the following fact. The exchange coupling in the second peak is so

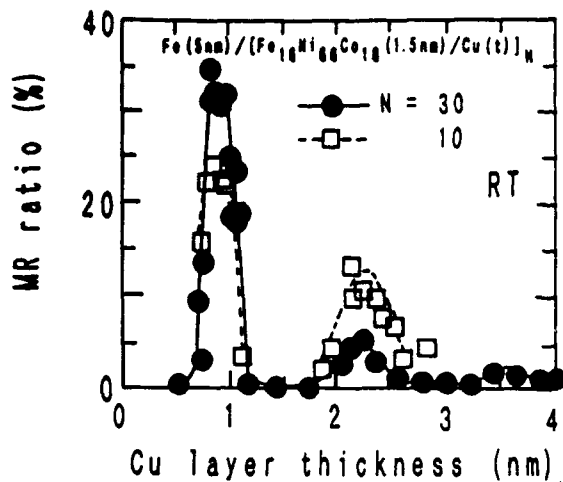
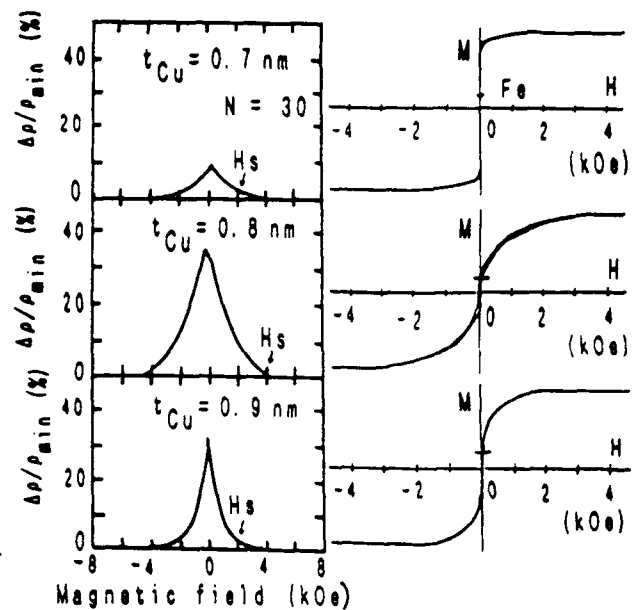


Fig. 1 The dependence of saturation MR ratio on Cu layer thickness at room temperature.

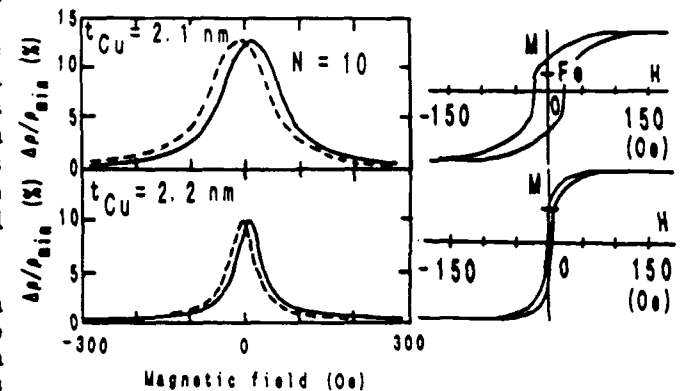
smaller that antiferromagnetic alignment becomes imperfect with increasing number of layers.

Fig. 2(a) and (b) show the hysteresis curves of MR and Magnetization around the first and the second peaks, respectively. In Fig. 2(a), the saturation field  $H_s$  in the magnetization curve for  $[\text{NiFeCo}(1.5\text{nm})/\text{Cu}(0.8\text{nm})]_{30}$  and  $[\text{NiFeCo}(1.5\text{nm})/\text{Cu}(0.8\text{nm})]_{10}$  multilayers are 2 kOe and 1 kOe, respectively, while MR ratios in both multilayers are nearly the same. In Fig. 2(b), the saturation field is only 100 Oe which is smaller by a factor 10 than those in the first peak. Comparing with  $(\text{FeNi}/\text{Cu}/\text{Co}/\text{Cu})$  multilayer, the  $H_s$  of  $\text{FeNiCo}/\text{Cu}$  at the 2nd peak is smaller by a factor 5 and the hysteresis effect in MR ratio is also much smaller. As seen from the MH curves, the remanent magnetization consists in samples with large magnetoresistance entirely of the magnetization of Fe buffer layer. Thus it is thought that each NiFeCo layer is perfectly antiferromagnetically aligned through the interlayer exchange coupling.

Fig. 3 shows the relation between the MR ratio and the interlayer coupling ratio,  $M(\text{AF})/M$ , defined from MH curves as shown in Fig. 3, where  $M$  is the saturation magnetization of NiFeCo multilayers and  $M(\text{AF})$  is the part of the magnetization thought to be aligned antiferromagnetically at zero field. If each magnetic layer aligns perfectly antiparallel, the net magnetization becomes zero at



(a) first peak



(b) second peak

Fig. 2 The hysteresis curves of MR and magnetization.

the remanence and  $M(\text{AF})/M$  should be 1. As shown in the figure, MR ratios at the first peak can be linearly extrapolated to 35%, when  $M(\text{AF})/M$  becomes 1. Thus the magnetoresistance value of the first peak obtained here is thought almost the maximum to be obtained in this system.

For technological applications, it is important that a large changes in the resistance occurs by the application of a weak magnetic field. Fig. 4 shows the Cu layer thickness dependences of the MR ratio and the interlayer magnetic coupling  $J$  given by

$$J = H_s M_F t_p / 4,$$
 where  $M_F$  and  $t_p$  are the saturation magnetization and thickness of the magnetic layers, respectively. The

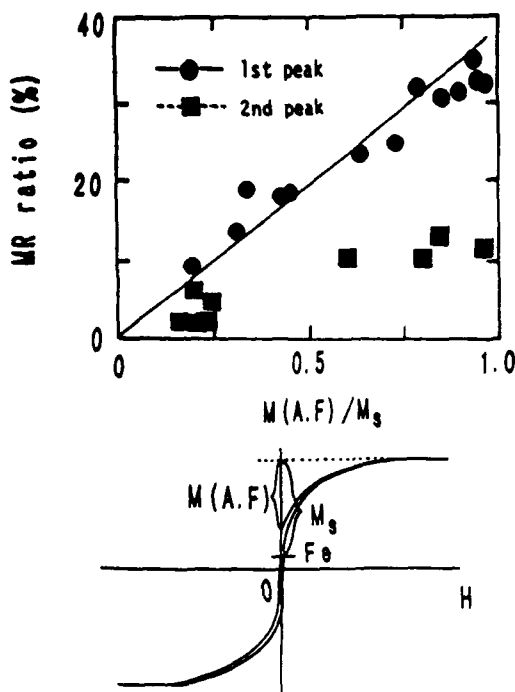


Fig.3 The relation between the MR ratio and the interlayer coupling ratio.

maximum interlayer coupling strength is approximately  $0.1 \text{ erg/cm}^2$  at room temperature. This value is smaller than that in Co/Cu and Fe/Cr multilayers. The coupling strength at the second peak is  $0.005 \text{ erg/cm}^2$ , which is smaller by a factor 20 than that at the first peak. From the figure, we can also find that the interlayer coupling strength is more sensitive to the Cu thickness than the MR ratio, especially around the first peak. Since at the second peak the saturation field  $H_s$  is as low as  $100 \text{ Oe}$ ,  $[\text{FeNiCo}(1.5\text{nm})/\text{Cu}(2\text{nm})]$  multilayers are expected to be applied in magnetic sensors.

#### 4. Summary

(FeNiCo/Cu) multilayers have the giant magnetoresistance at room temperature. The maximum value is about 35% and the oscillations in magnetoresistance are found. The saturation field and the interlayer coupling are more sensitive for Cu layer thickness than MR ratio. These facts suggest that very large MR ratio with a small saturation field can be obtained by optimizing the structure, composition and so on in this system.

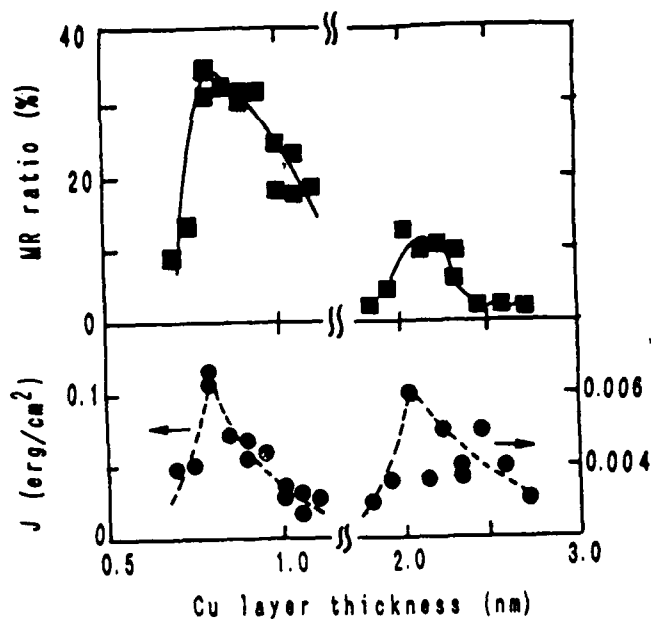


Fig.4 The Cu layer thickness dependences of the MR ratio and the interlayer coupling.

#### Acknowledgment

We thank Dr. Y.Hosoe of Central Research Lab., Hitachi, Ltd. for useful discussion and Mr.S.Goto for experimental assistant.

#### References

- [1] M.N.Baibich, J.M.Broto, A.Fert, F.Nguyen van Dau, F.Petroff, P.Etienne, G.Creuzet, A.Friederich and J.Chazelas: *Phys.Rev.Lett.*, 61, 2472 (1988)
- [2] S.S.P.Parkin, N.More and K.P.Roche: *Phys. Rev. Lett.*, 64, 2304 (1990)
- [3] D.H.Mosca, F.Petroff, A.Fert, P.A.Schroeder, W.P.Pratt, Jr and R.Laloe and S.Lequien: *J. Magn. & Magn. Mater.*, 94, L1 (1991)
- [4] S.S.P.Parkin, R.Bhadra and K.P.Roche: *Phys. Rev. Lett.*, 66, 2162 (1991)
- [5] T.Shinjo and H.Yamamoto: *J.Phys. Soc. Jpn.*, 9 3061 (1990)
- [6] B.Diney, V.S.Speriousu, S.S.P.Parkin, B.A.Gurney, D.R.Wilhoit and D.Mauri: *Phys. Rev. B*, 43, 1297 (1991)
- [7] L.W.McKeehan: *Phys.Rev.* 51, 136 (1937)  
C.H.Tolman: *J. Appl. Phys.*, 38, 3409 (1967)
- [8] S.S.P.Parkin: *Phys.Rev.Lett.*, 67, 3598 (1991)

# MAGNETORESISTANCE OF 82Ni-Fe/Al-Al<sub>2</sub>O<sub>3</sub>/Co JUNCTION

T. Miyazaki

*Department of Applied Physics, Tohoku University, Sendai 980, Japan*

Recently much effect has been paid on the giant magnetoresistance in artificial superlattices. The giant magnetoresistance effect attracts much attention not only from the point of view of physics, but also from the application of the superlattices as an electronic devices. The so called magnetic valve effect is very similar to the effect of giant magnetoresistance, and is expected to give a useful experimental support to interpret the giant magnetoresistance effect. Furthermore, the enhancement of magnetoresistance measured perpendicular to the film plane can be achieved by controlling the preparation condition of sandwich films.

In this meeting, we present the experimental result of magnetoresistance for 82Ni-Fe/Al-Al<sub>2</sub>O<sub>3</sub>/Co magnetic tunneling junction. Especially, the dependence of the conductance on the angle between the magnetizations of 82Ni-Fe and Co layers, and the temperature dependence of magnetoresistance will be described.

The typical cross-strip-electrode configuration was used. The first 1000 Å thick 82Ni-Fe layer (Permalloy) was evaporated onto a glass substrate in a form of 1×12 mm<sup>2</sup>. Then, a 150 Å thick Al layer was evaporated on the center of a Ni-Fe film in the circular form with a diameter of 2.5 mm. The surface of Al was oxidized in air at room temperature for 30 h. On the Al-Al<sub>2</sub>O<sub>3</sub> layer, a 1000 Å thick Co layer was evaporated in the rectangular form of 1×18 mm<sup>2</sup> perpendicular to the long axis of the Ni-Fe film.

Figs.1(a),(b) show the dependence of the resistance on the intensity of the magnetic field at room temperature. As seen in the figures, the resistance increases sharply at several oersted and keeps nearly constant up to about 65 Oe, followed by a decrease with further increasing the intensity of the magnetic field. The ratio  $\Delta R/R$  is about 2.7% even at room temperature.

Fig.2 shows hysteresis curve of the 82Ni-Fe/Al-Al<sub>2</sub>O<sub>3</sub>/Co film measured parallel to the long axis of the Co layer. Comparing figs.1 and 2, we can see clearly that the major and minor loops correspond well to those of the magnetoresistance curves.

Fig.3 shows the dependence of the tunneling conductance on the angle between the magnetizations of two ferromagnetic layers. It is seen that the conductance can be well expressed as  $G=G_0(1+\epsilon\cos\theta)$  which was recently derived theoretically by Slonczewski<sup>3</sup>.

Detail sample preparation method and other experimental results will be presented at the meeting.

## Reference

- 1) T. Miyazaki, T. Yaei and S. Ishio, *J. Magn. Magn. Mater.*, 98(1991) L1.
- 2) T. Yaei, S. Ishio and T. Miyazaki, *J. Magn. Soc. Jpn.*, (1992) (in press).
- 3) J.C. Slonczewski, *Phys. Rev.*, 39 (1989) 6995.

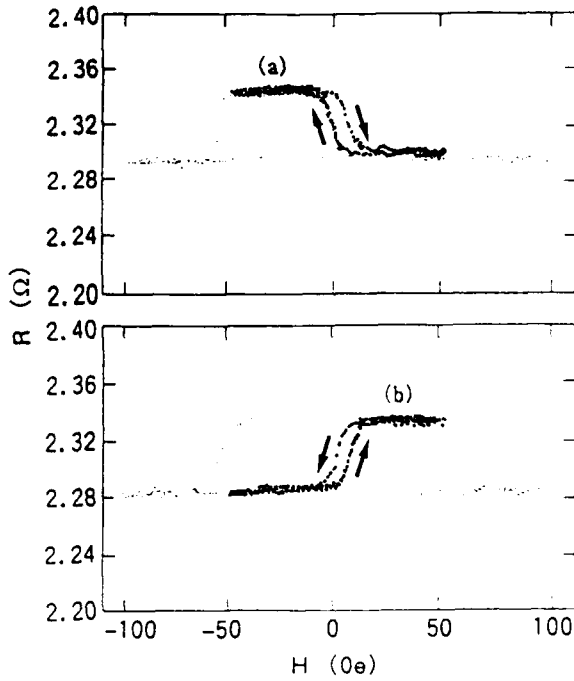


Fig.1 Resistance as a function of the magnetic field for the  $82\text{Ni-Fe/Al-Al}_2\text{O}_3\text{/Co}$  junction. Small dots are the resistance measured in alternating magnetic field up to  $\pm 100$  Oe. The small open circles are the resistance measured in fields between  $\pm 50$  Oe.

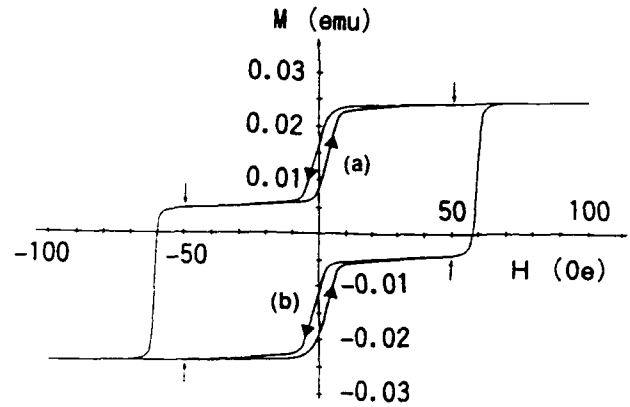


Fig.2 The magnetic hysteresis curve corresponding to the magnetoresistance curve in fig.1. The minor loops show the change of magnetization by alternating the magnetic field between the arrows in the figure.

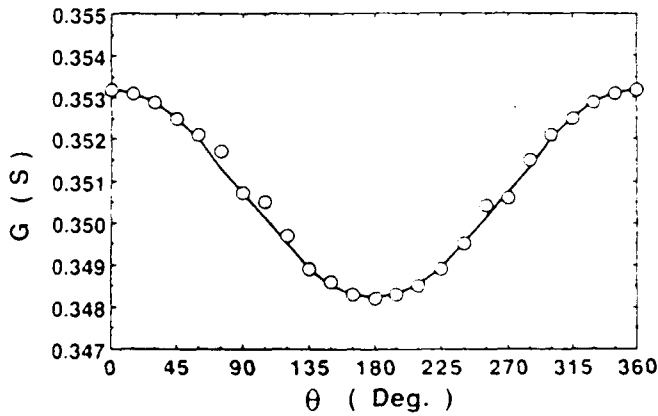


Fig.3 Dependence of the tunneling conductance ( $G$ ) on angle ( $\theta$ ) between the magnetizations of two ferromagnetic layers.

Magnetoresistance with Currents *Perpendicular*  
to the Plane of the Multilayers

W.P. Pratt Jr.

Department of Physics and Astronomy  
Michigan State University, E. Lansing, MI 48824, USA.

Two important parameters for understanding the Giant Magnetoresistance (MR) in ferromagnetic/normal metal (F/N) multilayers are the spin-orientation-dependent scattering rates in the bulk of F and at the F/N interfaces. Measurements with the current flowing in the layer planes (CIP-MR) have the advantage of being straightforward to make, but they have the disadvantage that it is difficult to separate scattering in the bulk of F from scattering at the F/N interfaces. In contrast, measurements with the current flowing perpendicular to the layer planes (CPP-MR) have the disadvantage of being more difficult to make, but they offer the potential of obtaining a better determination of these two scattering parameters, since in this direction the scattering of the electrons in the F and N layers and at the F/N interfaces is sequential.

We recently showed how to measure the CPP-MR<sup>1</sup> and found that, at least in Co/Ag multilayers, the CPP-MR is considerably larger than the CIP-MR, as predicted by Zhang and Levy.<sup>2</sup> However, for quantifying the two scattering rates mentioned above, analysis of the field-dependent CPP total resistance  $R_T$  of a multilayer is needed, rather than analysis of ratios of resistances used in the conventional definition of MR. This talk will emphasize the  $R_T$  analysis for the Co/Ag system primarily.

For CPP measurements<sup>1</sup> we place 1-mm-wide superconducting Nb strips on opposite sides of Co/Ag multilayers, giving an effective contact area through the sample of  $A = 1 \text{ mm}^2$  and  $R_T = 0.1 \mu\Omega$ . In my talk I will describe how our  $R_T$  measurements are made with a SQUID null detector with  $H \leq 1 \text{ kOe}$  and discuss the uncertainties in the data. Fig. 1 (a) and (b), respectively, illustrate the behaviors of  $AR_T$  and the magnetization  $M$  vs  $H$  for layer thicknesses  $t_{\text{Co}} = t_{\text{Ag}} = 6 \text{ nm}$  and define the three important magnetic fields that will be used in the analysis: field  $H_0 = 0$  for the as-prepared sample; the saturation field,  $H_S$ ; and the field  $H_M$  (= coercive field) at which the resistance of a given sample is maximum after cycling to  $H_S$ . Note that with  $t_{\text{Ag}} = 6 \text{ nm}$  the Co layers are magnetically "uncoupled." Because  $R_T$  of the sample includes the boundary resistances associated with the two Nb/multilayer contacts on opposite sides of the sample, our R-CPP measurements are effectively "two-terminal", and both the magnitude and possible  $H$  dependence of these contact resistances must be determined. Fig. 1 (c) shows the  $AR_T$  data for a Nb/Co/Nb sandwich with  $t_{\text{Co}} = 9 \text{ nm}$  where  $AR_T$  is dominated by these contact resistances. Fig. 1 (c) clearly shows that the total contact resistance is relative small ( $\approx 6 \text{ f}\Omega\text{m}^2$ ) and field independent. Thus our  $R_T(H)$  data are free of  $H$ -dependent systematic errors and can be corrected for these relative small  $H$ -independent contact resistances.

To analyze the  $AR_T(H)$  data at  $H_0$ ,  $H_M$  and  $H_S$ , I will use a simple series resistor model:

$$AR_T[H] = 2AR_{S/F} + M \left[ \rho_N t_N + \rho_F[H] t_F + 2AR_{F/N}[H] \right] \quad (1)$$

where  $M$  is the number of bilayers in a given sample,  $R_{S/F}$  is the contact resistance between the superconducting strip  $S$  and the multilayer,  $\rho_N$  is the resistivity of the  $N$  layer,  $\rho_F[H]$  is the effective  $H$ -dependent  $\rho$  of the  $F$  layer,  $R_{F/N}[H]$  is the effective  $H$ -dependent  $R$  of the  $F/N$  interface, and the approximation  $M-1 \approx M$  is used. For fixed total sample thickness,  $t = M(t_N + t_F) = 720$  nm, Eq. (1) can be rewritten for two cases:

Case #1:  $t_F = \text{constant}$ .

$$\begin{aligned} AR_T[H] &= \left[ 2AR_{S/F} + \rho_N t \right] + M \left[ (\rho_F[H] - \rho_N) t_F + 2AR_{F/N}[H] \right] \quad (2) \\ &= \text{INTERCEPT} + M \times \text{SLOPE} \end{aligned}$$

Case #2:  $t_F = t_N$ .

$$AR_T[H] = \left[ 2AR_{S/F} + (\rho_N + \rho_F[H]) (t/2) \right] + M \left[ 2AR_{F/N}[H] \right] \quad (3)$$

Figs. 2 and 3 show  $AR_T[H]$  for a series of Co/Ag multilayers with  $t_{Ag}$  large enough to magnetically decouple the Co layers, all sputtered under similar conditions onto cooled  $c$ -axis oriented single crystal sapphire substrates. In Fig. 2 the data points represent Case #1 with  $t_{Co} = 6$  nm. In Fig. 3 the data for Case #2 are shown. Both sets of data are consistent in form with the linear variations with  $M$  predicted by Eqs. (2) and (3), and the solid lines are fits of these equations to these data. The dotted lines in Fig. 1 represent best fits of Eq. (2) to the data (not shown) for  $t_{Co} = 2$  nm.

I will show that the agreement between the data for this series of Co/Ag samples and the series resistance model allows one to obtain numerical values of the  $H$ -dependent parameters  $\rho_{Co}[H]$  and  $AR_{Co/Ag}[H]$ . Data on Co/Ag multilayers prepared under different conditions, as well as data on Co/Ag(4%Sn) and Co/Cu multilayers, are being taken. As time permits, some of these will be compared with the data of Figs. 2 and 3 and with the simple series model.

This work was supported in part by NSF Grants DMR-88-013287 and DMR-91-22614 and by the MSU Center for Fundamental Materials Research.

## References

1. W.P. Pratt, Jr, S.-F. Lee, J.M. Slaughter, R. Loloee, P.A. Schroeder, and J. Bass, Phys. Rev. Letters 66, 3060 (1991).
2. S. Zhang and P.M. Levy, J. Appl. Phys. 69, 4786 (1991).

Figures

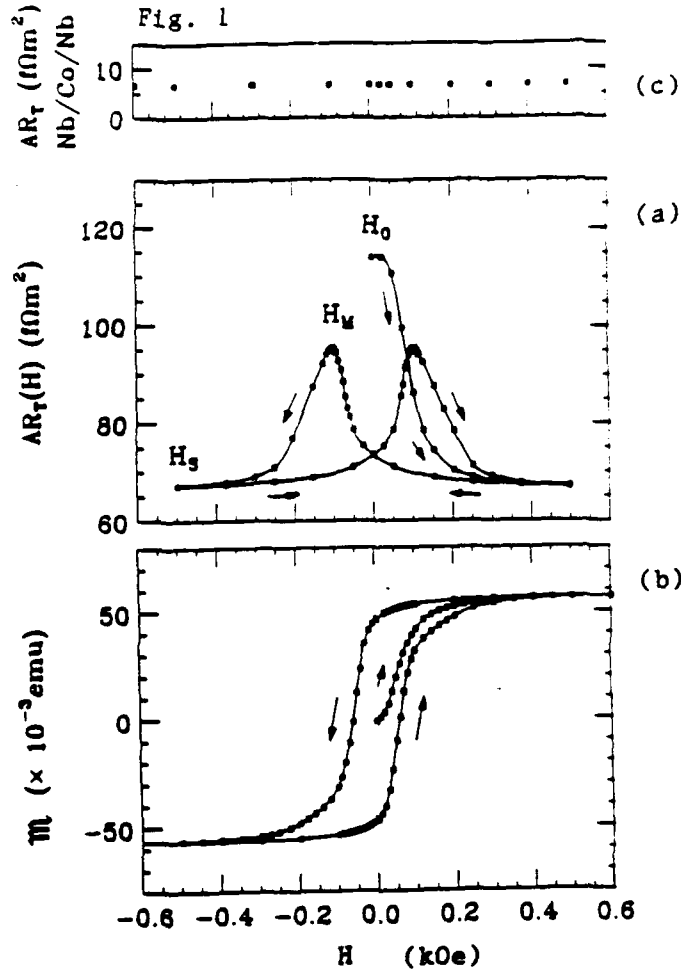


Fig. 2

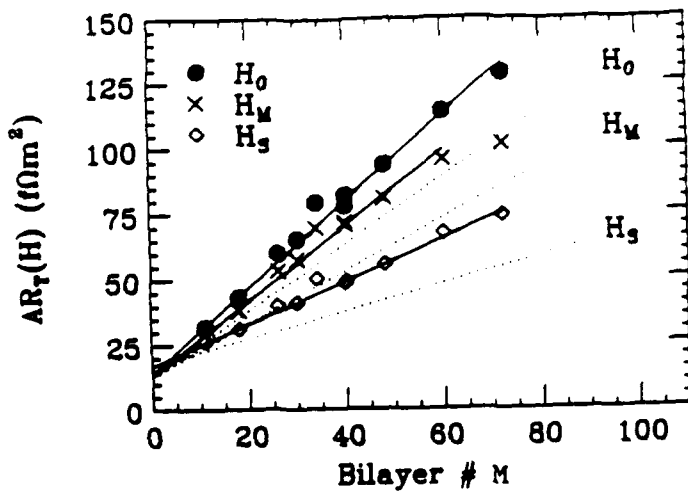
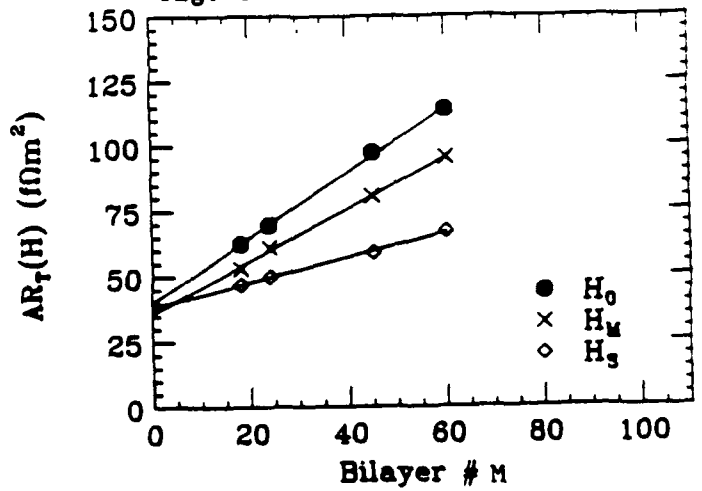


Fig. 3



## GIANT MAGNETORESISTANCE IN MAGNETIC MULTILAYERS AND SANDWICHES

S.S.P. Parkin

IBM Research Division, Almaden Research Center  
650 Harry Road, San Jose, California 95120-6099

The giant magnetoresistance effect in magnetic multilayers can attain enormous values of more than 65% at room temperature in Co/Cu multilayers containing thin Co and Cu layers 8-10 Å thick<sup>1,2</sup>. In such structures the saturation fields, which are determined by the antiferromagnetic exchange coupling of adjacent Co layers are large,  $\approx 10$  kOe. As the Cu layer thickness separating the Co layers is increased the magnitude of the saturation magnetoresistance oscillates between large and small values, paralleling oscillations in the magnetic coupling of the Co layers back and forth from antiferromagnetic to ferromagnetic coupling. The period of the oscillation is about 9-10 Å<sup>1</sup>. We find similar results for a wide variety of Cu based multilayers containing magnetic layers made up of Co, Fe, Ni, Ni<sub>1-x</sub>Fe<sub>x</sub> ( $x \approx 0.2$ ), and Co<sub>1-x</sub>Fe<sub>x</sub> ( $x = 0$  to 0.95). In each case the oscillation period is approximately the same but the phase of the oscillation depends on the structural integrity of the multilayer<sup>4,5</sup>.

For the Cu based multilayered systems the indirect magnetic exchange coupling mediated through the Cu layers decays rapidly with increasing Cu layer thickness, whereas the magnetoresistance (MR) decays slowly approximately as the inverse Cu layer thickness at low temperatures<sup>3</sup>. Thus very large values of MR, exceeding 30-35% at room temperature, are obtained for field changes of just 100-300 Oe in Co/Cu multilayers containing Cu layers, about 20 Å thick<sup>2,4,5</sup>. The magnitude of the MR is sensitive to the structural integrity of the multilayers, particularly for multilayers containing thin Cu layers, and is maximized in structures grown on Fe buffer layers<sup>1,2</sup>. This result has subsequently been confirmed by several other groups. The buffer layer plays a less important structural role for structures containing thicker Cu layers.

A variety of models have been proposed to explain the GMR phenomenon. These models differ in large part by the whereabouts of the spin dependent scattering of the conduction electrons, whether predominantly *interfacial*, from scattering near the interfaces of the magnetic and non-magnetic layers, or *bulk*-from scattering within the interior of the magnetic layers. We demonstrate the predominant role of interface scatter by showing that the addition of a single monolayer of Co at the permalloy/ Cu interfaces in NiFe/Cu/NiFe exchange biased sandwich structures doubles the magnetoresistance. Note that the magnetoresistance of NiFe/Cu multilayered structures is about half that of similar Co/Cu structures<sup>6</sup>. Thus we show it is the nature of the interface between the magnetic and non-magnetic layers which determines the magnitude of the MR and not the bulk nature of the magnetic layers. Indeed addition of Co at only one of the two NiFe/Cu interfaces results in an increase of the magnetoresistance by only half as much or about 50%. Moreover the increase in MR ob-

tained by dusting the NiFe/Cu interfaces with Co is insensitive to the thicknesses of the NiFe layers in the sandwich. Detailed measurements of the increase in the magnitude of the MR with the thickness of the Co interface layers gives length scales for the interfacial region of just 2.5 angstrom at room temperature and even smaller values of about half as much at 4.2 K. Such a diminution in length scale with temperature is consistent with interfacial but not bulk scattering. We find similar length scales in a wide variety of structures, both sandwiches and multilayers containing different magnetic and spacer layer materials demonstrating that the predominant role of interfacial scattering is a general property of the giant MR phenomenon in both sandwich and multilayered structures.

Finally we discuss the dependence of magnetoresistance on the non-magnetic spacer layer thickness. We present a simple phenomenological model which accounts for the thickness dependence over a very wide range of spacer layer thickness and use this model to determine the volume scattering within the spacer layer and its temperature dependence. We show that the temperature dependence of the MR is largely determined by scattering within the spacer layers in contradiction to many recently proposed models.

### **References:**

- [1] S.S.P. Parkin, R. Bhadra and K.P. Roche, Phys. Rev. Lett. **66**, 2152 (1991).
- [2] S.S.P. Parkin, Z.G. Li and D.J. Smith, Appl. Phys. Lett. **58**, 2710 (1991).
- [3] S.S.P. Parkin, A. Modak and D.J. Smith, Appl. Phys. Lett. (submitted).
- [4] S.S.P. Parkin, "Magnetic Surfaces, Thin Films and Multilayers", edited by S.S.P. Parkin *et al*, Mat. Res. Soc. Symp. Proc. **231**, 145 (1992).
- [5] S.S.P. Parkin, "Magnetic Surfaces, Thin Films and Multilayers", edited by S.S.P. Parkin *et al*, Mat. Res. Soc. Symp. Proc. **231**, 211 (1992).
- [6] S.S.P. Parkin, Appl. Phys. Lett. **60**, 512 (1992).

# Theory of Transport Properties in Magnetic Superlattices

Sadamichi Maekawa  
Department of Applied Physics,  
Nagoya University 464-01, Japan

In my talk, I would like to present three topics which we are currently studying in connection with the transport properties in magnetic superlattices: i) scattering mechanism of spin-dependent electric current in magnetic superlattices, ii) the transfer matrix formalism of the magneto-transport properties and the ferromagnetic tunneling, and iii) local electronic and magnetic structure of magnetic superlattices in the recursion method.

## i) Scattering mechanism of spin-dependent current.<sup>1-3)</sup>

Electrical resistivity in magnetic alloys has been one of the important subjects in solid-state physics for many years. In the alloys, the electric current is scattered by the spin-disorder so that the current is spin-dependent. However, it was not possible to observe each spin component of the current separately in the alloys. Here, we extend the theory of magnetic alloys to magnetic superlattices taking into account random exchange potential due to the disorder at the interfaces in the superlattices. We observe that in the superlattices each spin component of the current can be distinguished resulting in the large magneto-resistance. The material dependence of the magneto-resistance as well as the temperature dependence is examined. Based on the theoretical results, several possible superlattices showing the large magneto-resistance will be proposed.

## ii) The transfer matrix method in magnetic superlattices.<sup>4)</sup>

In the transfer matrix method, the conductance is given by the tight-binding model and the Landauer formula. This method has been applied to various quantum transport problems in small devices of metals and semiconductors. We extend this method to magnetic superlattices and ferromagnetic tunneling junctions and discuss quantum magneto-transport properties in these systems.

iii) Recursion method of the local electronic and magnetic structure.<sup>5)</sup>

Various novel magnetic as well as transport properties in magnetic superlattices are sensitively dependent on the properties at the interfaces. We calculate the local electronic and magnetic structure in  $TM/TM'$  superlattices,  $TM$  and  $TM'$  being transition metals, in the recursion method. We examine how local electronic structure depends on the disorder at the interfaces.

References:

- 1) J. Inoue, A. Oguri and S. Maekawa: J. Phys. Soc. Jpn. **60** (1991) 376.
- 2) J. Inoue and S. Maekawa: Prog. Theor. Phys. Suppl. **106** (1991) 187.
- 3) J. Inoue, H. Itoh and S. Maekawa: J. Phys. Soc. Jpn. **61** (1992) No.4.
- 4) A. Oguri, Y. Asano and S. Maekawa: to be published.
- 5) H. Itoh, J. Inoue and S. Maekawa: to be published.

# **Boltzmann Equation Approach to the Negative Magnetoresistance of Ferromagnetic-Normal Metallic Multilayers**

*L. M. Falicov and Randolph Q. Hood*

Department of Physics,  
University of California,  
Berkeley, CA 94720

and

Materials Sciences Division,-  
Lawrence Berkeley Laboratory,  
Berkeley, CA 94720

## *ABSTRACT*

The Boltzmann equation is solved for a system consisting of a ferromagnetic - normal - ferromagnetic metallic trilayer. The in-plane conductance of the film is calculated for two configurations: the ferromagnetic layers aligned (i) parallel and (ii) antiparallel to each other. The results explain the giant negative magnetoresistance encountered in these systems when an initial antiparallel arrangement is changed into a parallel configuration by application of an external magnetic field. The calculation depends on (A) geometric parameters (the thicknesses of the layers); (B) intrinsic metal parameters (number of conduction electrons, magnetization and effective masses in the layers); (C) bulk sample pro-

perties (conductivity relaxation times); (D) interface scattering properties (diffuse scattering versus potential scattering at the interfaces); and (E) outer surface scattering properties (specular versus diffuse surface scattering). For perfect specular scattering at the surfaces the problem becomes identical to an infinite multilayer, periodic system. It is found that a large negative magnetoresistance requires, in general, considerable asymmetry in the interface scattering for the two spin orientations. All qualitative features of the experiments are reproduced. Quantitative agreement can be achieved with sensible values of the parameters. The effect can be conceptually explained based on considerations of phase-space availability for an electron of a given spin orientation as it travels through the multilayer sample in the various configurations.

April 2, 1992

# Magnetoresistivity of Multilayers for Current in Plane and Perpendicular to the Plane of the Layers

Peter M. Levy, Horacio E. Camblong and Shufeng Zhang

Department of Physics, New York University, New York, NY 10003

Up to the present the emphasis on magnetoresistance (MR) in magnetic multilayered structures has been for currents in the plane of the layers, CIP. We have modelled the transport properties of metallic magnetic multilayered structures by considering conduction electrons subject to bulk scattering which occurs within the layers, and roughness scattering which occurs at the interfaces between layers. Due to the spatial and spin inhomogeneities in these structures, it is necessary to consider position dependent one and two point conductivities  $\sigma(z)$  and  $\sigma(z, z')$ . Therefore, for a uniform electric field *parallel* to the layers the current varies from one layer to another (as well as within the layers) and depends on the orientation of the magnetic moments; the measured conductivity is proportional to  $\iint \sigma(z, z') dz dz'$ . By using the Kubo formalism, we have succeeded in deriving the CIP conductivity for magnetic layered structures.<sup>1</sup>

For the current *perpendicular* to the plane of the layers, CPP, it is the electric field that varies from one layer to another; the measured *resistivity* in this direction is proportional to  $\iint \rho(z, z') dz dz'$ . In order to find the CPP resistivity and MR, one must either invert the

two point conductivity, or use a variational method in which one finds the internal electric field  $E(z')$  as well as the measured resistivity.<sup>2</sup> For CPP, unless otherwise constrained, one finds from the equation of continuity a *mixing* of the two currents, for conduction electrons with spin-up and spin-down, even though spin-flip scattering is not introduced in the model. This will be called CPP (2). In order to maintain two independent currents in the CPP direction, we introduce Lagrange multipliers; this leads to effective internal electric fields that are *different* for the two currents, CPP (1). Which model is applicable to a multilayered system depends on the amount of spin-flip scattering; we will discuss the scenarios under which the two models CPP(1) and CPP(2) apply.

In our original model,<sup>3</sup> we used the CPP(1) model and took the spin dependent effective electric field  $E^s(z)$  to be inversely proportional to the one point conductivity  $\sigma^s(z) = \int \sigma^{ss}(z, z') dz'$ . This leads us to a CPP conductivity which depends on the global amount of scattering in the multilayered structure and its overall state of magnetization, e.g.  $M=0$  or  $M=M_s$ , but which is independent of i) how the scattering is spatially distributed, and ii) the orientation of the magnetization of one layer relative to its neighbors. This leads to a CPP-MR which is strikingly different from the CIP-MR. The predictions based on this realization of CPP(1), have been largely confirmed by the recent CPP-MR experiments on Co/Ag multilayers at Michigan State University.<sup>4</sup> While these results lend support to the assumptions made in order to arrive at our original model, we are presently considering the CPP-MR by using the two point conductivity function.

We will present our fits to the CIP-MR and CPP-MR data on Co/Ag, and we will discuss new directions in the theory of giant magnetoresistance in magnetic layered

structures.

This work was supported in partly the Office of Naval Research and the New York University Technology Transfer Fund.

References:

1. P.M. Levy et al., J. Appl. Phys. **67**, 5914 (1990); P.M. Levy, S. Zhang and A. Fert, Phys. Rev. Lett. **65**, 1643 (1990); Phys. Rev. B **45**, 8689 (1992).
2. H. Camblong, to be published.
3. S. Zhang and P.M. Levy, J. Appl. Phys. **69**, 4786 (1991).
4. W.P. Pratt, Jr., S.-F. Lee, J.M. Slaughter, R. Loloee, P.A. Schroeder and J. Bass, Phys. Rev. Lett. **66**, 3060 (1991), and to be published.

## **Interlayer Coupling**

# Magneto-Optic Characterizations of Superlattices and Wedged Sandwiches with Oscillatory Interlayer Magnetic Coupling\*

S. D. Bader

Materials Science Division, Argonne National Laboratory, Argonne, IL 60439

Longitudinal magneto-optic Kerr-effect measurements have been used to characterize sputtered Fe/Cr superlattices [1] and to discover that Fe/Mo [2] and Fe/Nb [3] superlattices also belong to the new class of materials that have oscillatory interlayer magnetic coupling. All three superlattice systems are based on *bcc* spacer layers that are (110) textured. Fe/Mo and Fe/Nb provide instructive contrast to the Fe/Cr system. For example, under the same sputter-growth conditions, x-ray-diffraction characterization shows that Fe/Mo has superior structural qualities, including observation of up to seven orders of low-angle x-ray diffraction peaks and an rms roughness of only 2Å. Fe/Mo, however, yields a magnetoresistivity at the first antiferromagnetic peak that is more than an order of magnitude *lower* than that of Fe/Cr. Fe/Nb exhibits as many as five antiferromagnetic oscillations, with a period of 9.9Å of Nb, yields an interfacial roughness estimate from analysis [4] of the high-angle x-ray diffraction peaks that is similar to that for Fe/Mo, yet possesses a magnetoresistivity that is only one-fifth as large as that for Fe/Mo.

Additional transport characterizations were performed for the sputtered Fe/Cr superlattice system. Three antiferromagnetic oscillations were detected in the magnetoresistivity [1], as was reported previously. The magnetothermopower shows complementary behavior at room temperature [5]. Analysis of the temperature dependence of the magnetoresistivity shows the influence of the thermal excitation of magnons. The magnetoresistivity of antiferromagnetic films decay from a maximum at low temperature with a  $T^2$ -behavior below 100K, while ferromagnetic films follow approximately a  $T^{3/2}$ -behavior [1]. These power laws are expected for the thermal occupation of anisotropic-antiferromagnetic and ferromagnetic magnons, respectively. The temperature dependencies of the magnetization follow similar power-law behaviors, while the non-coupled case with 100Å-thick Cr spacer layers follow an approximately linear T-behavior, as anticipated [6].

In contrast to studies on polycrystalline superlattices, sandwiches with wedged spacer layers were grown by means of molecular beam epitaxy (MBE). Structural and growth characterizations were obtained from low- and high-energy electron diffraction and Auger spectroscopy. Epitaxial Fe/Mo/Fe was grown on Mo(100) because the (100) orientation represents the nesting direction of Mo. In this case the theoretically anticipated short-period oscillations were observed, and a periodicity of ~3 monolayers (ML) was obtained [7]. Figure 1 shows representative magneto-optic Kerr loops obtained *in situ* by scanning a focused laser across Mo wedges that separate two 14ML-thick Fe films. The laser position is expressed in units of Mo thickness at the right of Fig. 1. For the first antiferromagnetic regions the switching is rather abrupt, and indicative of only two stable orientations of the magnetization of the two Fe films: parallel and antiparallel. The switching field  $H_S$ , represented by the offset in the centroid of the loop from zero, is initially larger than the coercivity; but  $H_S$  decreases as the Mo spacer layer thickens and causes subsequent antiferromagnetically-coupled loops to exhibit full remanence. The switching fields are plotted in Fig. 2. Five antiferromagnetic regions are observed in Fig. 2 with an ~3-ML period. (When  $H_S=0$ , the interlayer coupling is either ferromagnetic or zero.)

Mo represents a simplification over Cr since there are no magnetic moments associated with Mo spacer layers. However, Mo is still a complex transition metal with a challenging Fermi surface. To introduce additional simplicity, wedged sandwiches of Co/Cu/Co were grown by MBE on Cu(100). This system was chosen because its magnetic and structural properties had been studied previously. Symmetric sandwiches with three different Co thicknesses  $d_{\text{Co}}$  were studied in a similar manner to that applied to the Fe/Mo/Fe system. Three oscillations were detected with a periodicity of 5.5ML (or 9.9Å) of Cu [8]. The  $H_S$  values were used to estimate  $J_{\text{AF}}$ , the interlayer coupling energy in the antiferromagnetic case, using the familiar expression  $J_{\text{AF}} = M_S H_S d_{\text{Co}}$ , where  $M_S$  is the saturation magnetization. Figure 3 shows a summary of the results. The most important feature of Fig. 3 is the demonstration that  $J_{\text{AF}}$  is independent of  $d_{\text{Co}}$ . Although this is an anticipated result, it is one that is important to verify, because it implies that the coupling occurs at the interface and is independent of the Co thickness. Theoretical models that represent each magnetic layer in the sandwich or superlattice as a monolayer implicitly make such an assumption.

---

\* Work supported by the U.S. Department of Energy, Basic Energy Sciences-Materials Sciences under contract W-31-109-ENG-38.

- [1]. J.E. Mattson, Mary E. Brubaker, C.H. Sowers, M. Conover, Z. Qiu, and S.D. Bader, "Temperature Dependence of the Magnetoresistance of Sputtered Fe/Cr Superlattices", Phys. Rev. B 44, 9378 (1991).
- [2]. Mary E. Brubaker, J.E. Mattson, C.H. Sowers, and S.D. Bader, "Oscillatory Interlayer Magnetic Coupling of Sputtered Fe/Mo Superlattices", Appl. Phys. Lett. 58, 2306 (1991).
- [3]. J.E. Mattson, C.H. Sowers, A. Berger, and S.D. Bader, "Magnetoresistivity and Oscillatory Interlayer Magnetic Coupling of Sputtered Fe/Nb Superlattices", (submitted).
- [4]. E.E. Fullerton, J.E. Mattson, M.E. Brubaker, C.H. Sowers, and S.D. Bader, "Structural Refinement of Fe/Nb and Fe/Mo Superlattices by X-ray Diffraction", [Abstract] Bull. Amer. Phys. Soc. 37, 404 (1992).
- [5]. M.J. Conover, M.B. Brodsky, J.E. Mattson, C.H. Sowers, and S.D. Bader, "Magnetothermopower of Fe/Cr Superlattices", J. Magn. Magn. Mater. 102, L5 (1991).
- [6]. Z.Q. Qiu, J.E. Mattson, C.H. Sowers, U. Welp, S.D. Bader, H. Tang, and J.C. Walker, "Temperature Dependence of the Magnetization of Superlattices with Variable Interlayer Magnetic Couplings", Phys. Rev. B (1992) 1 April, in press.
- [7]. Z.Q. Qiu, J. Pearson, A. Berger, and S.D. Bader, "Short-Period Oscillations of the Interlayer Magnetic Coupling of Wedged Fe(100)/Mo(100)/Fe(100) Grown on Mo(100) by Molecular Beam Epitaxy", Phys. Rev. Lett. 68, 1398 (1992).
- [8]. Z.Q. Qiu, J. Pearson, and S.D. Bader, "Oscillatory Interlayer Magnetic Coupling of Wedged Co/Cu/Co Sandwiches Grown on Cu(100) by Molecular Beam Epitaxy", submitted.

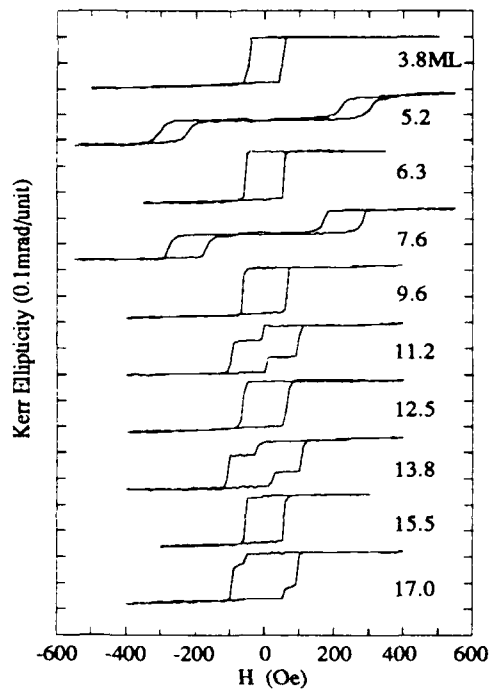


Fig. 1: Kerr loops for Fe/Mo/Fe grown epitaxially on Mo(100), for 14-ML Fe films and Mo wedge thickness shown.

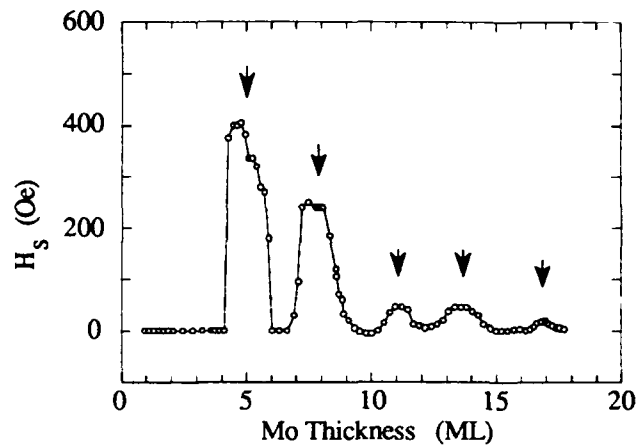


Fig. 2: Switching fields obtained from Fig. 1, showing short-period oscillations.

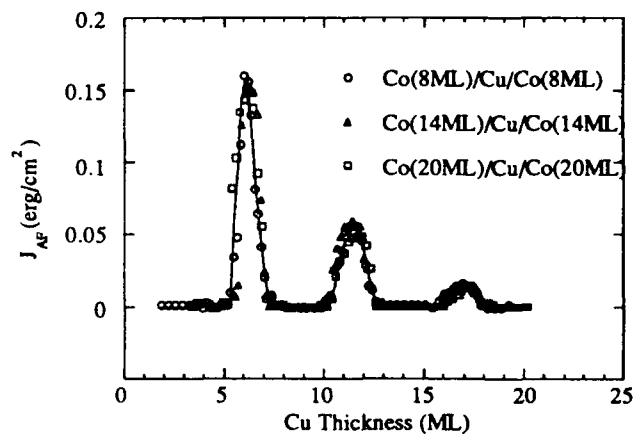


Fig. 3: Antiferromagnetic coupling strength for Co/Cu/Co sandwiches grown on Cu(100) with wedged Cu spacer layers. The coupling strength is independent of the Co thickness.

The submitted manuscript has been authored by a contractor of the U. S. Government under contract No. W-31-109-ENG-38. Accordingly, the U. S. Government retains a nonexclusive, royalty-free license to publish or reproduce the published form of this contribution, or allow others to do so, for U. S. Government purposes.

## EXTENDED ABSTRACT

### Oscillations of the Exchange Coupling in Fe/Cr/Fe(100) and Fe/Ag/Fe(100)

D.T. Pierce, J. Unguris, and R.J. Celotta  
National Institute of Standards and Technology, Gaithersburg, MD

The exchange coupling between magnetic layers separated by nonmagnetic layers oscillates between ferromagnetic and antiferromagnetic coupling as a function of spacer layer thickness in a wide variety of systems.<sup>1</sup> In a few systems more than one period of oscillation has been observed. The origin of the coupling and the factors that determine the period of the oscillations in the coupling are subjects of intense discussion, as is the technologically important spin-valve magnetoresistance observed in multilayers of these materials. This work aims to provide precise determinations of the oscillation periods in the highest quality structures possible in order to test theoretical models.

Results are reported for two different sandwich structures where the spacer layers are respectively a transition metal, Cr, and a noble metal, Ag. This is the first observation of coupling through Ag which had previously been reported not to exhibit coupling. In each case, the spacer layer is grown in a wedge of linearly increasing thickness as shown in Fig. 1. The domains in the top Fe layer are imaged by Scanning Electron Microscopy with Polarization Analysis (SEMPA). The high spatial resolution of the SEM allows us to use the small, nearly perfect Fe single crystal whisker substrate. The relevant region of the clean Fe whisker has the simple two-domain structure shown schematically.

The period of the oscillations in Cr was observed to depend very sensitively on the film structure.<sup>2</sup> The domains in the top Fe layer of two Fe/Cr/Fe sandwiches, in which the Cr wedge was evaporated onto the substrate at 250° C and at room temperature, are displayed in the top and bottom panels of Fig. 2 respectively. The black (white) regions correspond to the magnetization pointing to the right (left, +M<sub>y</sub>) in the figure. The long period oscillations have a period of 10 to 12 layers or 1.5-1.8 nm. The short period oscillations, on the other hand, have a period of approximately 2.1 layers. Reflection High Energy Electron Diffraction (RHEED) patterns showed that the Cr grown on a room temperature substrate has some roughness and disorder while the growth at 250° C is of a quality similar to the substrate. Clearly, the magnetic coupling is very sensitive to the film structure. Such short period oscillations with a sensitivity to interface roughness were predicted by Wang et al.<sup>3</sup>

A precise determination of the interlayer thickness is possible by counting the spatial RHEED intensity oscillations, where one oscillation corresponds to a thickness change of one layer, as the SEM beam is moved along the wedge. This is analogous to the conventional measurement of the oscillation in the specular RHEED intensity as the film thickness changes with time during growth. The RHEED oscillations are shown in Fig. 3, lined up with a line

profile of the magnetization taken through the top of Fig. 2. Three defects, noted by solid dots, are observed in both the RHEED oscillations and the SEMPA magnetization image allowing the registry of the "atomic ruler" provided by the RHEED oscillations with the oscillations in the magnetic coupling. The magnetic coupling is seen to reverse with each layer of Cr thickness with a period of 2 layers. Careful comparison of the RHEED and magnetic oscillations reveals a "phase slip" at 22-23 layers indicating the period of the magnetic coupling is incommensurate with the lattice period. We have grown thicker wedges and have observed over 37 short period magnetic oscillations through over 10 nm of Cr. For such long wedges, three phase slips are observed, each separated by 20 layer spacings, indicating a period of 2.1 layers.

In the case of Ag, the best growth was obtained with the Fe substrate at 60-100° C, but RHEED patterns indicated that the Ag layers were not as structurally perfect as the highest quality Cr layers. Nevertheless, after a thickness of about 5 layers, spatial RHEED oscillations were observed allowing a precise determination of the period of the oscillation of the magnetic coupling in Ag. Magnetic coupling was observed through thicknesses of Ag exceeding 10 nm. A SEMPA image of the oscillations in the magnetic coupling in a Fe/Ag/Fe(100) sandwich is shown in Fig. 4. Two short period oscillations are directly observed at 14 and 26 layers thickness. Indirect evidence for the influence of a short period oscillation is given by the variation in the length of the long period oscillations as shown in the figure.

Much of the theoretical effort to date has gone toward explaining the most widely observed long period oscillations. The observation of both long and short period oscillations places additional demands on the theories. The well known RKKY interaction, which has explained magnetic coupling through rare earth layers, has the asymptotic form for coupling between two planes of magnetic moments of  $(k_z z)^{-2} \sin(k_z z)$ , where  $z$  is the distance between the planes and  $k_z$  is an extremal Fermi surface spanning vector of the spacer layer material. The periods  $L=2\pi/k_z$  are related directly to the Fermi surface spanning vectors. The short period oscillations in Cr are caused by the strong Fermi surface nesting wavevector  $k_z=0.95\pi/d$ , where  $d$  is the layer spacing. This same nesting wavevector is the cause of the spin density waves in Cr. Another less strongly nested wavevector can be found which corresponds to the long period oscillations, but then there are many other weakly nesting wavevectors spanning the rich Cr Fermi surface for which magnetic oscillations have not been found.

In the case of Ag, which has a nearly spherical Fermi surface with necks at the L points, only two Fermi surface spanning vectors are identified in the [100] direction appropriate to the experimental geometry.<sup>4</sup> One is the  $2k_F$  that spans the Fermi "sphere" of Ag which gives a period of  $5.6d$  and the other is a wavevector at the neck which gives a period of  $2.4d$ , where for Ag,  $d=0.204$  nm. A model in which two sine waves with periods of 2.4 and 5.6 layers are superposed is consistent with the SEMPA measurement displayed in Fig. 4.

In summary, it is clear from these measurements that the magnetic coupling depends sensitively on the structure of the layers. From our SEMPA measurements of Cr and Ag as spacer layers between Fe, it appears that the periods of the magnetic coupling oscillations are unique to each spacer material and there are strong indications that the periods are determined to a first approximation by Fermi surface spanning vectors.

This work was supported in part by the Office of Naval Research.

### References

1. S.S.P. Parkin, Phys. Rev. Lett. **67**, 3598 (1991).
2. J. Unguris, R.J. Celotta, and D.T. Pierce, Phys. Rev. Lett. **67**, 140 (1991)
3. Y. Wang, P.M. Levy, and J.L. Fry, Phys. Rev. Lett. **65**, 2732 (1990).
4. P. Bruno and C. Chappert, Phys. Rev. Lett. **67**, 1602 (1991).

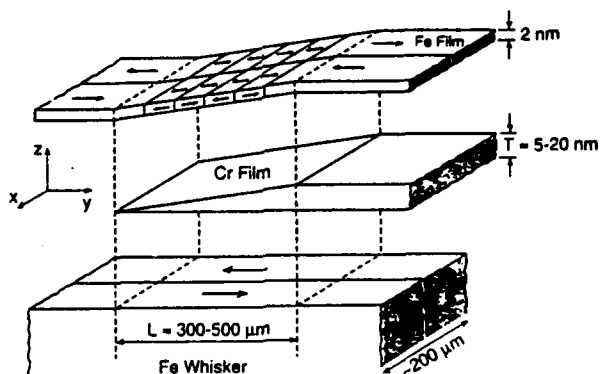


Fig. 1

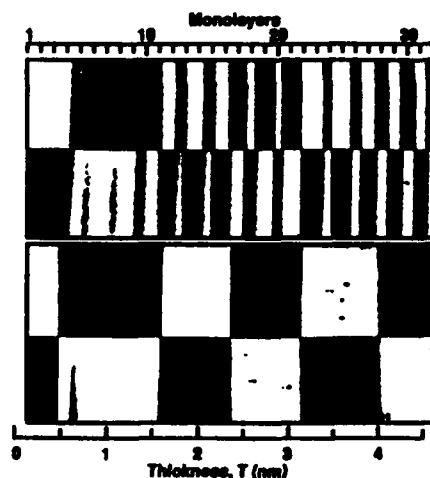


Fig. 2

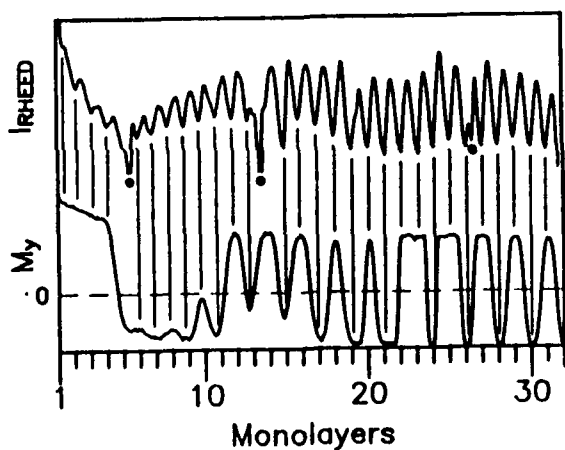


Fig. 3

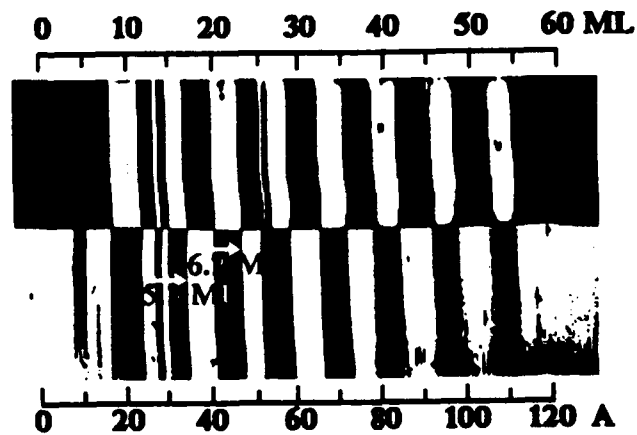


Fig. 4

# **STRONG TEMPERATURE DEPENDENCE OF THE 90° COUPLING IN Fe/Al/Fe(001) MAGNETIC TRILAYERS**

**G.A. Prinz\***

**Naval Research Laboratory  
Washington, DC 20375**

The coupling of ferromagnetic films through a non-magnetic interlayer has become an important theme in solid state magnetism following the ground-breaking papers by Grünberg et al.[1] and Fert et al.[2]. The early work revealed a bilinear exchange coupling energy per unit area of the form

$$E_C = - 2A_{12}(M_1 \cdot M_2). \quad (1)$$

where  $M_1$  and  $M_2$  are unit vectors along the magnetic moments of the two magnetic layers. These vectors lie 180° apart in zero field if  $A_{12}$  is negative. Recently, it was found that, in certain cases, one also requires a biquadratic coupling mechanism of the form [3]

$$E_C' = - 2B_{12}(M_1 \cdot M_2)^2 \quad (2)$$

to explain the data. For negative  $B_{12}$ , the moments in the two layers prefer to lie at 90° to one another, in plane, in zero applied field. This effect was originally observed [3,4] in the Fe/Cr/Fe(001) system at those Cr thicknesses where  $A_{12} \approx 0$ . More recently, 90° coupling has been observed in the Fe/Al/Fe(001) system [5], where it can be comparable in strength to the 180° coupling, and also in Co/Cu/Co(001) [6].

The temperature dependence of the 180° coupling has been studied in several laboratories for the Fe/Cr/Fe system with

consistent results [7-11]. The coupling constant  $A_{12}$  falls slowly and nearly linearly with increasing temperature, extrapolating to zero near 1000 K. This result has been interpreted to be a consequence of the two-dimensional nature of the coupled system [10], and such behavior also has been observed in the other bilinearly coupled system measured to date [11].

In this paper, we report the temperature dependence of the  $90^\circ$  coupling in the Fe/Al/Fe(001) system. It is qualitatively different from the approximately linear dependence seen for the  $180^\circ$  coupling, falling off very rapidly as the temperature of the system is raised. The recent theoretical model by Slonczewski [12], which was constructed to explain the  $90^\circ$  coupling seen in Fe/Cr/Fe, showed that the  $90^\circ$  term can result from static fluctuations in the  $180^\circ$  term caused by interface roughness. However, we show that this mechanism does not appear able to explain the temperature dependence of the  $90^\circ$  coupling found here for Fe/Al/Fe(001).

[1] P. Grünberg, R. Schreiber, Y. Pang, M.B. Brodsky, and H. Sowers, *Phys. Rev. Lett.* **57**, 2442 (1986); F. Saurenbach, U. Walz, L. Hinchey, P. Grünberg, and W. Zinn, *J. Appl. Phys.* **63**, 3473 (1988).

[2] M.N. Baibich, J.M. Broto, A. Fert, F. Nguyen Van Dau, F. Petroff, P. Etienne, G. Creuzet, A. Friederich, and J. Chazelas, *Phys. Rev. Lett.* **61**, 2472 (1988).

[3] M. Ruhrig, R. Schafer, A. Hubert, R. Mosler, J.A. Wolf, S. Demokritov, and P. Grünberg, *Phys. Stat. Solidi (a)* **125**, 635 (1991).

- [4] J. Unguris, R.J. Celotta, and D.T. Pierce, *Phys. Rev. Lett.* **67**, 140 (1991).
- [5] A. Fuss, S. Demokritov, P. Grünberg, and W. Zinn, *J. Magn. Magn. Mater.* **103**, L221 (1992)
- [6] B. Heinrich, J.F. Cochran, M. Kowalewski, J. Kirschner, Z. Celinski, A.S. Arrott, and K. Myrtle, *Phys. Rev. B* **44**, 9348 (1991).
- [7] A. Chaiken, T.M. Tritt, D.J. Gillespie, J.J. Krebs, P. Lubitz, M.Z. Harford, and G.A. Prinz, *J. Appl. Phys.* **69**, 4798 (1991).
- [8] A. Barthelemy, A. Fert, M.N. Baibich, S. Hadjoudj, F. Petroff, P. Etienne, R. Cabanel, S. Lequin, F. Nguyen Van Dau, and G. Creuzet, *J. Appl. Phys.* **67**, 5908 (1990).
- [9] S. Demokritov, J.A. Wolf, P. Grünberg, W. Zinn, *Proc. Spring 1991 MRS Mtg., Anaheim, CA.*
- [10] J.R. Cullen and K.B. Hathaway (to be published).
- [11] S.S.P. Parkin, R. Bhadra, and K.P. Roche, *Phys. Rev. Lett.* **66**, 2152 (1991).
- [12] J.C. Slonczewski, *Phys. Rev. Lett.* **67**, 3172 (1991).

\*Work supported by the Office of Naval Research and carried out in collaboration with C.J. Gutierrez, J.J. Krebs and M.E. Filipkowski.

# Ferrimagnetic Behavior of Exchange-Coupled RE/TM Multilayers: Low-Field Spin-Flop and Magnetoresistance

K. Takanashi, H. Fujimori and Y. Fujiguchi  
*Institute for Materials Research, Tohoku University,  
Katahira, Aoba-ku, Sendai 980, JAPAN*

## 1. Introduction

Recent development of thin film preparation techniques has made it possible to control the magnetic structure artificially by multilayering on an atomic scale. Rare earth (RE)/ 3d transition metal (TM) multilayers are attractive materials in this respect, since novel magnetic structures are expected due to the exchange interaction between RE and TM magnetic moments at the interfaces. As described in a previous paper,<sup>1)</sup> Fe/Gd multilayers behave as 'giant' ferrimagnets, that is, magnetic moments of Fe and Gd layers couple in antiparallel with a long period of the order of  $10\text{--}10^2\text{\AA}$ . Consequently, the spin-flop in a low field and compensation behavior of magnetization can be observed. In addition, we have found that longitudinal ( $\rho_l$ ) and transverse ( $\rho_t$ ) magnetoresistances exhibit a crossover accompanied with the spin-flop. In the present study, these ferrimagnetic phenomena of magnetization and magnetoresistance have extensively been investigated. Particularly, systematic comparison between the experimental data and the calculated results by using a molecular field model will be presented. Furthermore, we will report the spin-flop of magnetization and the crossover of  $\rho_l$  and  $\rho_t$  at room temperature in Fe/Gd *double structured* multilayers, the results of which are important for the application to magnetoresistance devices.

## 2. Experimental procedure

Fe/Gd multilayers were prepared by rf sputtering. The multilayer period  $\lambda$  was designed in the range from 20 to  $200\text{\AA}$ . The ratio of the Fe layer thickness ( $t_{\text{Fe}}$ ) to the Gd layer thickness ( $t_{\text{Gd}}$ ) was 1.24:1 and the total thickness was about  $5000\text{\AA}$  for each sample.

In the case of Fe/Gd *double structured* multilayers, two types of Fe/Gd submultilayers with a shorter period  $\lambda_s$  were stacked alternately with a longer period  $\lambda_l$ . One type of Fe/Gd submultilayer has dominant Fe layer magneti-

zation at 0K with  $t_{\text{Fe}}:t_{\text{Gd}}=3:1$ , and the other has dominant Gd layer magnetization at 0K with  $t_{\text{Fe}}:t_{\text{Gd}}=1:3$ . The following two series of Fe/Gd *double structured* multilayers were prepared: a)  $\lambda_s$  was designed in the range from 4 to 100Å, keeping  $\lambda_l$  to 250Å; b)  $\lambda_l$  was designed in the range from 90 to 490Å, keeping  $\lambda_s$  to 20Å. The total thickness was about 3000Å.

The standard X-ray diffraction measurement using FeK $\alpha$  radiation was made for structural determination. The magnetization was measured using a vibrating sample magnetometer as a function of the temperature from 4.2K to room temperature (RT) and of the applied field up to 20kOe. The magnetoresistance was measured at 77K and RT in the maximum applied field of 9kOe by a conventional four-terminal method.

### 3. Structure, magnetization and magnetoresistance of Fe/Gd multilayers<sup>1,2)</sup>

The multilayer periodicity in Fe/Gd multilayers has been confirmed from low-angle X-ray diffraction. Bragg peaks corresponding to the multilayer period are observed up to considerably high orders, suggesting the existence of definite compositional modulation. High-angle X-ray diffraction indicates that Fe/Gd multilayers are polycrystalline with poor crystallinity.

The spin-flop behavior of magnetization is definitely observed at 4.2 and 77K in the samples with  $\lambda$  larger than about 60Å, and is not observed at RT. For example, the magnetization vs. applied field (M-H) curves for  $\lambda=67$ Å are shown in Fig. 1. The M-H curve reveals a pattern characteristic of the spin-flop at 4.2 and 77K, while at RT, a simple pattern as is often observed for ordinary ferromagnets. We consider that the Gd layer magnetization disappears at RT, and hence the spin-flop cannot be observed. Figure 2 shows the magnetization vs. temperature (M-T) curves in the samples with various  $\lambda$ 's. The compensation behavior is seen for  $\lambda=67$  and 90Å, and not for other samples. Thus, the temperature region with dominant Fe (or Gd) layer magnetization depends strongly on  $\lambda$ . This suggests that the Fe and/or Gd moments have magnitudes different from those in bulk metals, and depend on  $\lambda$ .

The magnetic structure in ferrimagnetic multilayer films can be calculated within a molecular field approximation.<sup>3-6)</sup> We have evaluated the magnetizations at various temperatures and in various applied fields from the calculated magnetic structure in Fe/Gd multilayers. In the calculation, we assumed that the composition was modulated stepwise, and that the exchange

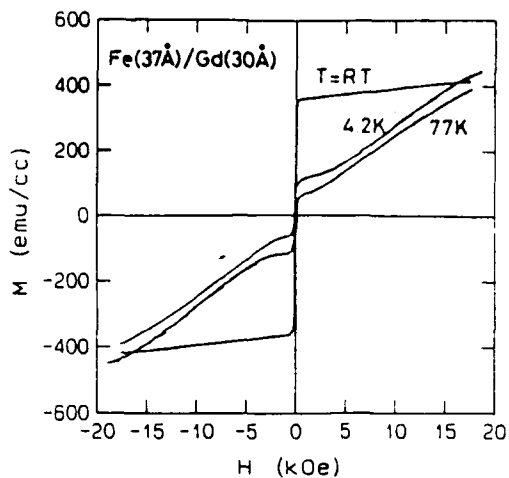


Fig. 1 The M-H curves of the Fe/Gd multilayer with  $\lambda=67\text{\AA}$ .

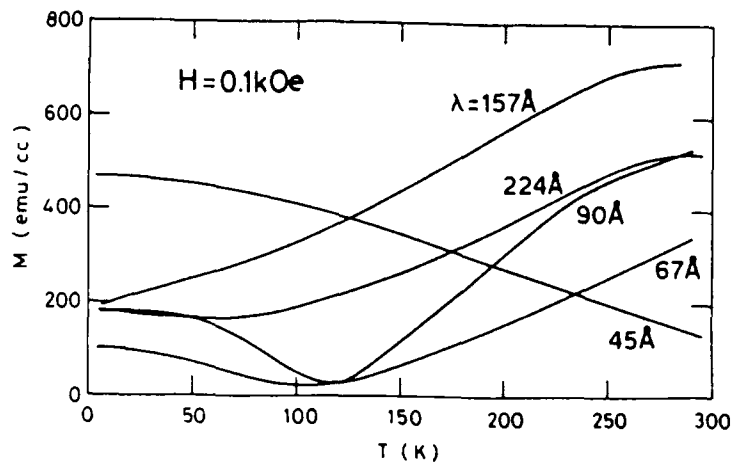


Fig. 2 The M-T curves of Fe/Gd multilayers with various  $\lambda$ 's.

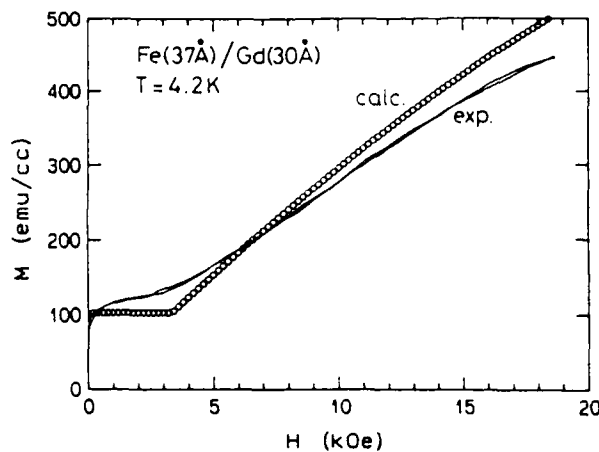


Fig. 3 (a) The experimental and calculated M-H curves at 4.2K for the Fe/Gd multilayer with  $\lambda=67\text{\AA}$ .

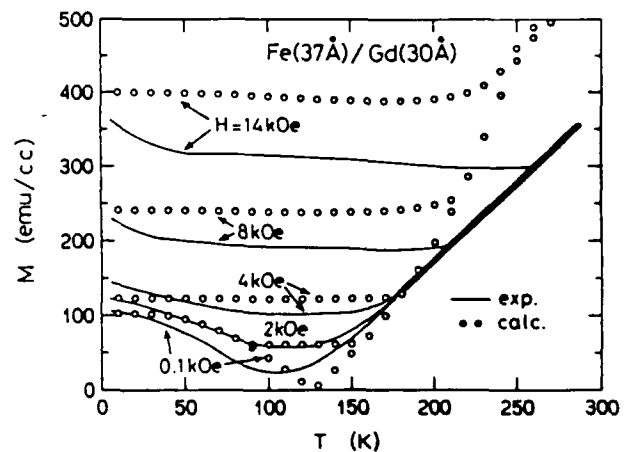


Fig. 3 (b) The experimental and calculated M-T curves in various applied fields for the Fe/Gd multilayer with  $\lambda=67\text{\AA}$ .

interaction in Fe and Gd layers were the same values as those in bulk Fe and Gd metals. The magnitudes of Fe and Gd moments were determined so as to be consistent with the magnetization before the spin-flop. It has been suggested that the magnitude of Fe moments decreases with decreasing  $\lambda$ , which is considered to be due to the compositional mixing near the interface and/or the amorphous-crystalline transition.<sup>7)</sup> In spite of many assumptions, the calculated M-H and M-T curves have been found to agree fairly well with the experiments. As a typical example, experimental and calculated M-H and M-T curves for  $\lambda=67\text{\AA}$  are shown in Figs. 3 (a) and (b), respectively.

The measured magnetoresistance reveals a crossover of  $\rho_l$  and  $\rho_t$  around

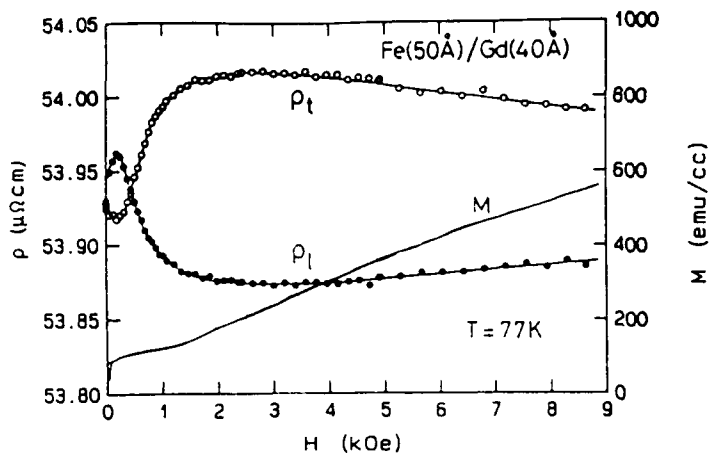


Fig. 4 The  $\rho_l$  and  $\rho_t$  vs.  $H$  curves at 77K for the Fe/Gd multilayer with  $\lambda=90\text{\AA}$ , compared with the  $M-H$  curve.

the spin-flop field ( $H_{sf}$ ) as is shown in Fig. 4. This phenomenon is considered to be due to the rotation of the magnetic moments accompanied with the spin-flop, since the electrical resistance depends on the angle between the directions of the electric current and of magnetic moments. Assuming parallel flow of the electric current in Fe and Gd layers, the magnetoresistance behavior can be simulated by using the calculated magnetic structure. We have found that the crossover of  $\rho_l$  and  $\rho_t$  is well reproduced in the calculation.

#### 4. Structure, magnetization and magnetoresistance in Fe/Gd double structured multilayers<sup>8-10)</sup>

The crossover of  $\rho_l$  and  $\rho_t$  in Fe/Gd multilayers suggests the possibility of their application to magnetoresistance devices. From the application point of view, it is important to obtain the spin-flop of magnetization and/or the crossover of  $\rho_l$  and  $\rho_t$  at RT. The Gd layer magnetization in Fe/Gd multilayers almost disappears at RT for large  $\lambda$  because the Curie temperature of Gd is close to RT, and consequently  $H_{sf}$  also disappears at RT. For small  $\lambda$ , on the other hand, the Gd layer magnetization remains alive even at RT due to the molecular field from the Fe layer magnetization. However,  $H_{sf}$  is considerably large because  $H_{sf}$  increases rapidly with decreasing  $\lambda$ .<sup>2-6)</sup> Thus, it is difficult to tune  $H_{sf}$  at RT to an appropriate value for application. As one approach for this problem, we proposed a new type of design of multilayers, that is, an Fe/Gd *double structured* multilayer.<sup>8)</sup> It is considered in Fe/Gd *double structured* multilayers that the Gd layer magnetization is alive at RT when  $\lambda_s$  is small, and that  $H_{sf}$  is sufficiently low when  $\lambda_l$  is large.

The *double structured* multilayer periodicity was confirmed from low-

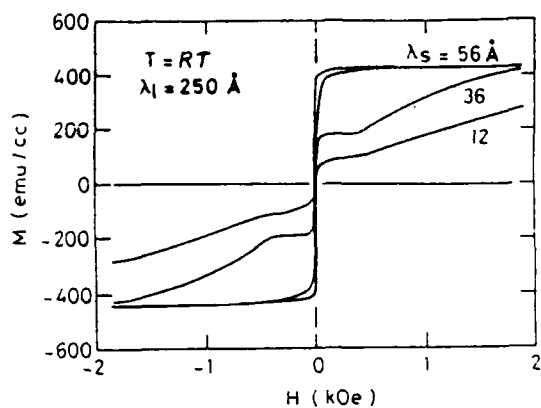


Fig. 5 The M-H curves at RT for Fe/Gd double structured multilayers with  $\lambda_1 = 250 \text{ \AA}$  and various  $\lambda_s$ 's.

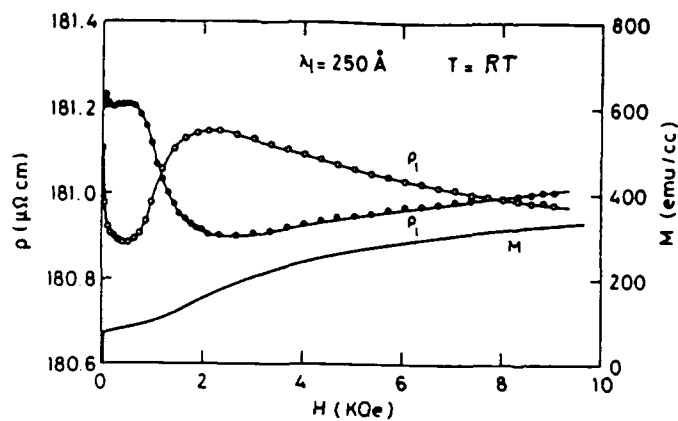


Fig. 6 The  $\rho_1$  and  $\rho_t$  vs. H curves at RT for the Fe/Gd double structured multilayer with  $\lambda_1 = 250 \text{ \AA}$  and  $\lambda_s = 20 \text{ \AA}$ , compared with the M-H curve.

angle X-ray diffraction. The calculated diffraction patterns based on the step model agree fairly well with the experimental results.

The magnetization of Fe/Gd double structured multilayers with  $\lambda_s$  smaller than  $56 \text{ \AA}$  reveals a spin-flop at RT in applied fields lower than 1 kOe, as is shown in Fig. 5. It has been found that  $H_{sf}$  at RT becomes lower than 100 Oe by choosing  $\lambda_s$  where the compensation temperature approaches RT and/or by choosing large  $\lambda_1$ . The crossover of  $\rho_1$  and  $\rho_t$  at RT is observed around  $H_{sf}$ . For example, Fig. 6 shows the  $\rho_1$  and  $\rho_t$  vs. applied field curve for the sample with  $\lambda_s = 20 \text{ \AA}$  and  $\lambda_1 = 250 \text{ \AA}$ , compared with the M-H curve.

## 5. Summary and conclusion

The magnetization of Fe/Gd multilayers reveals spin-flop and compensation behavior. The magnetoresistance shows a crossover of  $\rho_1$  and  $\rho_t$  accompanied with the spin-flop. Such ferrimagnetic phenomena can be simulated fairly well by the calculation based on the molecular field model. It is possible to tune  $H_{sf}$  to a desired value by choosing appropriate  $\lambda_s$  and  $\lambda_1$  in Fe/Gd *double structured* multilayers.

## Acknowledgment

We would like to thank Mr. Y. Hayakawa for collaboration in overall experiments. We are indebted to Professor M. Motokawa who collaborated in the calculation based on the molecular field model. This work was supported by a Grant-in-Aid for Scientific Research from the Ministry of Education, Science and Culture.

## References

- 1) Y. Kamiguchi, Y. Hayakawa and H. Fujimori: Appl. Phys. Lett. 55 (1989) 1918.
- 2) K. Takanashi, Y. Kamiguchi, H. Fujimori and M. Motokawa: J. Phys. Soc. Jpn. submitted.
- 3) R. E. Camley and D. R. Tilley: Phys. Rev. B37 (1988) 3413.
- 4) R. E. Camley: Phys. Rev. B39 (1989) 12316.
- 5) M. Motokawa: Prog. Theor. Phys. Suppl. No.101 (1990) 537.
- 6) M. Motokawa and H. Dohnomae: J. Phys. Soc. Jpn. 60 (1991) 1355.
- 7) J. Landes, Ch. Sauer, B. Kabius and W. Zinn: Phys. Rev. B44 (1991) 8342.
- 8) H. Fujimori, Y. Kamiguchi and Y. Hayakawa: J. Appl. Phys. 67 (1990) 5716.
- 9) Y. Kamiguchi, H. Fujimori, Y. Hayakawa and K. Takanashi: Nihon-*dyōj*ikigakkaishi (J. Magn. Soc. Jpn.) 14 (1990) 355 [in Japanese].
- 10) H. Fujimori, Y. Kamiguchi, Y. Hayakawa and K. Takanashi: MRS Symp. Proc., Anaheim, 1991, Vol.231 (MRS, Pittsburgh, 1992) pp.125-130.

# Spin Configurations in Rare-Earth, Rare-Earth/Transition Metal and other Magnetic Superlattices

R. E. Camley, Department of Physics, University of Colorado at Colorado Springs,  
Colorado Springs, CO 80933-7150

## Introduction

Magnetic metallic multilayers have show a stimulating richness of behavior. In particular we have seen a set of structures involving rare-earth and transition metal elements (Dy/Y, Gd/Y,<sup>1,2</sup> Gd/Dy<sup>3</sup>, Fe/Cr<sup>4</sup>, Co/Ru<sup>5</sup>, and Fe/Gd<sup>6</sup>) which exhibit a one or more magnetic phase transitions at relatively low temperatures and applied fields. In this talk, we first review some methods for calculating the magnetic structures and some earlier results on Fe/Gd<sup>7</sup> and Gd/Dy<sup>3</sup>. We then present some new results on surface phase transitions in Fe/Cr or Gd/Y type structures and on superlattices composed of antiferromagnets.

The phase transitions in these magnetic multilayers are primarily driven by a competition between interface exchange energy and Zeeman energy. Here we show that the multilayer structure can be **designed** to have a large number of different magnetic states depending on the layering pattern, the temperature, and the applied field. In addition we see that macroscopic properties of the superlattice, such as net magnetization and static susceptibility, depend strongly on the microscopic spin structure.

Several theoretical models<sup>8</sup> have been developed for dealing with phase transitions in magnetic multilayers. These include a Landau-Ginzburg approach, a microscopic, iterative, energy minimization approach, and the examination of the dynamic spin wave modes in order to find a "soft mode" which indicates a phase transition. The theoretical models, particularly the energy minimization approach, are shown to give a good account for the magnetization as a function of temperature for Gd/Dy, Gd/Y and Gd/Fe multilayers systems.

## Individual Systems -- Fe/Gd and Gd/Dy

The Fe/Gd superlattice is composed of two ferromagnets which couple antiferromagnetically at the interface. If the net magnetic moment in the Gd films is larger than that of the Fe films the Gd moments will line up with an external field and the Fe moments will be antiparallel to the field. We call this the Gd-aligned state. However when the moments in the Fe and Gd films are approximately equal, the system undergoes a phase transition to a twisted or canted state where the Fe and Gd spins are not aligned with the external field. The field required for this transition can be easily varied by varying the thickness of the Fe and Gd layers. If the layers are very thin then the critical field is fairly high. As the thickness is increased the critical field is reduced. The static susceptibility in the twisted state is much higher than in the aligned state because of the additional freedom associated with the orientation of the magnetic moments in the Gd and Fe films.

The Gd/Dy system is particularly interesting in that in some phases it displays a doubled magnetic unit cell, i.e. the magnetic unit cell is twice the size of the chemical unit cell. We show that this is due to a **collective effect** where the layered structure allows new configurations. In addition the Gd/Dy system also exhibits **interface effects** where the interface contributions profoundly influence the properties of the entire structure.

## Surface Phase Transitions

The Fe/Gd multilayer is quite interesting in that it displays a surface phase transition<sup>9</sup>. This transition corresponds to the spins in the outermost films being in the twisted state while the spins in the bulk of the multilayer are still in the aligned state. We show that this surface phase transition depends critically on the choice of the outermost film. If the outer film is Gd, then there is no surface phase transition. If the outer film is Fe then there is a surface phase transition which occurs at a critical magnetic field which is about 5 times smaller than that necessary to cause a bulk phase transition from the aligned to twisted state.

A slightly different surface phase transition can be found in Gd/Y and Fe/Cr systems. These structures can show antiferromagnetic coupling between the ferromagnetic films depending on the thickness of the nonmagnetic spacer layer. When this occurs an application of an external magnetic field in the plane of the layers causes the magnetic structure to go into a canted state which resembles the spin-flop state of an antiferromagnet. We have recently completed a study<sup>10</sup> of **finite** multilayers of this type and found that the canting angle, the deviation of the magnetization from the applied field, near the surface of the multilayer can vary significantly from the canting angles in the bulk of the multilayer. For example when the bulk canting angle is about 80° the canting angles near the surface can vary from 45° to 120°. The penetration depth of the surface phase can be quite large. In fact it extends to infinity for both very large and very small fields so that the surface distortion involves the entire sample. A variational calculation gives an approximate expression for the number of unit cells,  $L$ , over which the surface twist extends. In the low field limit we obtain a simple expression:

$$L = 1 + \sqrt{\frac{12}{h^2} - 1} \quad \text{where } h = \frac{H_0 M}{|J|}$$

Here  $h$  is a measure of the Zeeman energy compared to the exchange energy.  $H_0$  is the applied field;  $M$  is the net magnetic moment for a film and  $J$  is the interface exchange energy. In our results we find that the surface canting angle is always considerably smaller than the bulk canting angle. This suggests a possible method for experimental verification of the surface twist structure. If  $L$  is not too large, a measurement of the net magnetic moment of the superlattice will give a good approximation of the bulk canting angle. However a measurement of the magneto-optical Kerr effect (MOKE) is sensitive to the magnetic moment near the surface and could give a good account of the surface canting angle.

## Related Systems -- Antiferromagnetic Superlattices

In addition to the rare-earth and rare-earth/transition metal superlattices discussed above, there is now a significant body of experimental results on a variety of other systems. These include superlattices composed of antiferromagnets. Very recently the first experimental results<sup>11</sup> on the properties of antiferromagnetic superlattices (CoF<sub>2</sub>/FeF<sub>2</sub>) were reported. Bulk CoF<sub>2</sub> has a magnetic transition at about 40 K while bulk FeF<sub>2</sub> has a phase transition at a higher temperature of 78 K. The experiments showed that for superlattices with thicker films both high and low temperature magnetic phase transitions occur. Superlattice samples with thinner films showed only one (high temperature) magnetic phase transition.

The experimental results can be understood in terms of interface exchange coupling and film thickness. The key idea is that the coupling at the interfaces allows the material with the higher transition temperature to stabilize the material with the lower transition temperature. Since the stabilization only extends a few atomic layers away from the interface, this produces a significant effect for thin films, but only a small change for thicker films. Using the iterative model described above we have obtained good theoretical agreement with experimental results<sup>12</sup>. From our parameters we conclude that the magnetic films have fairly strong exchange coupling at the interface.

## References

- 1) J. Kwo et al, Phys. Rev. B **35** 7925 (1987) and Phys. Rev. Lett. **55**, 1402 (1985), and C. F. Majkrzak et al Phys. Rev. Lett. **56** 2700 (1986).
- 2) M. B. Salamon et al, Phys. Rev. Lett. **56** 259 (1986), J. J. Rhyne et al, J. Appl. Phys. **61**, 4043 (1987)
- 3) R. E. Camley et al, Phys. Rev. Lett. **64**, 2703 (1990)
- 4) P. Grünberg et al, Phys. Rev. Lett. **57**, 2442 (1986)
- 5) S. S. P. Parkin et al, Phys. Rev. Lett. **64**, 2304 (1990)
- 6) H. Fujimori et al, J. Appl. Phys. **67**, 5716 (1990) and K. Cherifi et al Phys. Rev. B **44** 7733 (1991)
- 7) R. E. Camley, Phys. Rev. B **39**, 12316 (1989)
- 8) R. E. Camley and D. R. Tilley, Phys. Rev. B **37**, 3413 (1988)
- 9) J. G. LePage and R. E. Camley, Phys. Rev. Lett. **65**, 1152 (1990)
- 10) F. C. Nörtemann, R. L. Stamps, A. S. Carriço, and R. E. Camley (submitted-Phys. Rev. B)
- 11) C. A. Ramos et al, Phys. Rev. Lett. **23**, 2913 (1990)
- 12) A. S. Carriço and R. E. Camley (submitted to Phys. Rev. B and in press Solid State Comm.)

## Simple theory of exchange coupling in transition metal magnetic multilayers

D.M. Deaven, D.S. Rokhsar\*

*Department of Physics, University of California, Berkeley, CA 94720*

M. Johnson

*Bell Communications Research, Red Bank, NJ 07701*

*Abstract:* Experiments on a variety of magnetic multilayer and sandwich structures reveal an indirect exchange coupling between layers of ferromagnets separated by nonmagnetic spacer layers. This coupling oscillates from ferromagnetic to antiferromagnetic depending on the thickness of the spacer layers, with an anomalously long period. We present a simple model to explain the long period and compare our results with the Ruderman-Kittel-Kasuya-Yosida (RKKY) theory of indirect exchange coupling.

The discovery of “giant magnetoresistance” in MBE-grown Fe/Cr multilayers[1] conjures up a cornucopia of technological applications and has spurred the study of other magnetic/nonmagnetic metallic multilayers. The “giant magnetoresistance” has now been observed in sputtered multilayers composed of essentially any of the transition metals [2], and MBE-grown multilayers of Fe/Cu[3,4]. In addition to anomalous transport properties, many of these systems share long period oscillations in the exchange coupling  $\mathcal{J}(r)$  between ferromagnetic layers as a function of nonmagnetic spacer layer thickness  $r$ . In general, these measurements show that  $\mathcal{J}(r)$  oscillates around zero for  $r$  in the range  $0 - 50\text{\AA}$ . Considering the strength of the coupling[2] ( $|\mathcal{J}| \sim 5 \text{ erg/cm}^2$  in Co/Ru, for example), some sort of indirect exchange mechanism must be operating; magnetostatic interactions are an order of magnitude too small. The period of the oscillation varies ( $\lambda \sim 7\text{\AA}$  in Fe/Cu and  $\lambda \sim 18\text{\AA}$  in Fe/Cr) but is substantially longer than the period predicted by a naive application of the Ruderman-Kittel-Kasuya-Yosida (RKKY) theory of indirect exchange coupling[5]. In the RKKY theory the period is fixed at the reciprocal of twice the Fermi wavevector, *i.e.*, a lattice constant.

Is this coupling simply related to the RKKY interaction, or does it represent a new type of indirect mechanism? We present[6] a calculation of  $\mathcal{J}(r)$  within a simple mean-field model of itinerant electrons. The  $\mathcal{J}(r)$  calculated using this model has a long period of oscillation. We also calculate the corresponding RKKY coupling, and show that our result is indeed a close cousin of the RKKY phenomenon. Our simple model incorporates tight-binding bands in both the magnetic and nonmagnetic layers, as well as a phenomenological exchange interaction within the magnetic layers. Thus we take into account the itinerant nature of the layers, as well as including a non-perturbative coupling between the magnetic and non-magnetic layers. We find that  $\mathcal{J}(r)$  exhibits a long oscillation period,  $\lambda \sim 4 - 6$  atomic layers, similar to that found experimentally. This result may be understood within the context of RKKY theory as a *short* period RKKY oscillation which is sampled at a uniform set of discrete points, corresponding to the number of atomic planes in a nonmagnetic spacer layer. This aliasing effect must be considered in any theory of exchange-coupled multilayers.[7]

When aliasing occurs, small changes of phase in the background short period oscillations can lead to large changes of phase in the aliased long period oscillations. Under these circumstances, an RKKY coupling which is *always* ferromagnetic in the small distance limit can lead to a coupling across *one* spacer layer which is either ferromagnetic or antiferromagnetic. This is consistent with the fact that both behaviors are observed experimentally.

The RKKY approach should only be formally valid in the limit of thin, weakly ferromagnetic layers interacting with host conduction electrons via contact interactions. Nevertheless, we have found that such a perturbative calculation can capture the qualitative features of a fully interacting model even in a regime where perturbation theory must break down. Perturbation theory is still correct in predicting the real-space asymptotic *period* (given the aliasing effect) and decay envelope of the exchange coupling. The *magnitude* of the RKKY prediction is, of course, too large, since the prefactor of the RKKY range function saturates near unity. The ability of this simple approach to predict the period (if not the magnitude) of multilayer coupling in simple models is encouraging, because it suggests that a quantitative perturbation theory may apply to the real materials.

Work at Berkeley was supported by the NSF under grant DMR-89-14440. D.S.R. acknowledges a grant from the Alfred P. Sloan Foundation.

### References

- [1] M.N. Baibich, *et al.*, *Phys. Rev. Lett.* **61**, 2472 (1988).
- [2] S. Parkin, *Phys. Rev. Lett.* **67**, 3598 (1991).
- [3] B. Heinrich, Z. Celinski, J.F. Cochran, W.B. Muir, J. Rudd, Q.M. Zhong, A.S. Arrot, and K. Myrtle, *Phys. Rev. Lett.* **64**, 673 (1990).
- [4] W.R. Bennett, W. Schwarzacher, and W.F. Egelhoff, Jr., *Phys. Rev. Lett.* **65**, 3169 (1990).
- [5] M.A. Rudermann and C. Kittel, *Phys. Rev.* **96**, 99 (1954); T. Kasuya, *Prog. Theo. Phys.* **16**, 45 (1956); K. Yosida, *Phys. Rev.* **106**, 893 (1957).
- [6] D.M. Deaven, D.S. Rokhsar, and M. Johnson, *Phys. Rev. B* **44** 5977 (1991).
- [7] Similar aliasing ideas can be found in D.M. Edwards, J. Mathon, R.B. Muniz and M.S. Phan, *Phys. Rev. Lett.* **67**, 493 (1991), and P. Bruno and C. Chappert, *Phys. Rev. Lett.* **67**, 1602 (1991),

## **Growth and Quantitative Studies of the Exchange Coupling In [Fe(001) whisker/Cr(001)/Fe(001) Structures.**

B. Heinrich, J.F. Cochran, M. From

Physics Department, Simon Fraser University, BURNABY, V5A1S6.

The strength of the exchange coupling through [Fe(001) whisker]/Cr(001)/6ML Fe(001) systems was investigated. The main purpose of these studies is to determine quantitatively the strength of the exchange coupling and to investigate the role of the interface roughness.

### **Growth studies:**

Fe(001) whiskers are known to be the best substrates with wide atomic terraces exceeding  $1\mu\text{m}$ . The growth mode depends very strongly on the substrate temperature. The growth of Fe(001) and Cr(001) below 100 C proceeds in a quasi layer by layer mode in which the surface roughness is mostly confined to the last two atomic layers but with a short terrace width of 40-60 Å. The Cr(001) and Fe(001) growths on Fe(001) and Cr(001) templates respectively show a well defined split in the RHEED pattern streaks at temperatures below 100 C. The shape of observed streak splitting is characteristic to the intersection of the Ewald sphere with reciprocal rods consisting of alternating segments of hollow cylinders and straight lines. The RHEED specular beam spot of the Fe(001) layers exhibits significantly stronger intensity when it is located centrally between split streaks. The corresponding RHEED intensity oscillations are in this case either very weak or even absent. These observations suggest that the central portion of the split streaks corresponds to the constructive interference (Bragg condition). The RHEED streak splitting is characteristic of the lateral spacing which in this growth is determined by the average spacing between atomic islands (terraces). The inverse value of the observed RHEED splitting leads an average terrace separation of 60 Å at room temperature.

The growth of Cr on Fe whisker substrates was carried out in a similar manner as was done by the NIST group. The substrate temperature during the growth of Cr on Fe(001) whiskers was varied between 250-400 C. An extensive investigation of the Cr growth was carried out by using Reflection High Energy Electron Diffraction (RHEED) with the electron beam impinging at large angles (2nd anti-Bragg

condition). Fe whiskers have no mosaic spread and therefore the width of diffracted beams is limited only by the instrumental resolution (several 1000 Å along the diffracted beam) and therefore one can investigate in detail the coherence length of grown overlayers and the average terrace size of their surfaces. In all growths the starting Fe(001) surface possesses the best surface. The long range coherence in Cr layers is maintained well at all studied substrate temperatures. However the average terrace width of Cr overlayers is very dependent on the substrate temperature. Only above 300 C the Cr overlayers start to exhibit respectable long atomic terraces. However even at 400 C low intensity streak tails are noticeable. The specular beam RHEED spot profiles indicate that the streak accompanying the central sharp diffracted beam is strongly affected by Kikuchi bands, and therefore the interpretation of RHEED streak lineshapes in terms of the average terrace size has to be taken with caution. One could argue that a mere presence of the RHEED streaks suggests that the Cr(001) surfaces are never as perfect as the starting Fe(001) whisker template. Although the growth of Cr at higher substrate temperatures (above 300 C) proceeds in a very good layer by layer growth mode. The RHEED intensity oscillations are very strong throughout the whole growth with no noticeable decrease of RHEED intensity oscillations even for high RHEED electron beam impinging angles. In fact the growth at 400 C substrate temperature shows clear cusps in the intensities which appears only when a new atomic layer is nucleated after the previous atomic layer is filled. The specular beam profile during the growth shows all features of a good layer by layer growth. The central sharp peak corresponding to the intersection of the Ewald sphere with the reciprocal rod changes its intensity very strongly during the growth. At the RHEED intensity maxima it reaches its maximum value while the intensity of the accompanying streak reaches its minima. At the minima of RHEED intensity oscillations the specular spot disappears entirely and the streaky portion of the diffracted beam reaches its maximum intensity. Such behavior was observed previously only in III/V compound structures, and clearly shows that the RHEED intensity oscillations are mostly dominated by the electron interference pattern between the top two atomic layers. The absence of the central specular beam at RHEED intensity minima proves that at this stage of the growth the the top Cr(001) atomic is half filled. One expects in this case a very effective averaging of the short wavelength exchange coupling.

#### Magnetic measurements:

The studies on Fe whiskers were carried out mostly by means of Brillouin Light Scattering (BLS) and some measurements were done using SMOKE. The exchange coupling was studied in [Fe(001) whisker/Cr(001)/6ML Fe(001)/10ML Ag(001)/20ML Au(001) samples with an variable Cr thickness. Since our emphases were put on the quantitative aspects of the exchange coupling we did not employ standard wedged samples. In any particular growth we prepared either two or three

samples with the Cr interlayers having their thicknesses increased by one atomic layer.

In BLS studies three resonance peaks were observed: the surface mode and the spin-wave manifold of Fe(001) whisker and the resonance mode corresponding to the 6ML Fe(001) which is coupled to the Fe(001) whisker. The Ag(001) layer was used to decrease the effective demagnetizing field,  $4\pi M_s$ , in 6ML Fe(001) layer in order to move its resonance frequency from the Fe(001) whisker spin-wave manifold.

The strength of the exchange coupling was determined by the following features:

(a) The field dependence of the 6ML resonance peak. In the antiferromagnetic coupling the field dependence of the resonance peak shows a softening of the resonance mode when the external field reaches the critical field required to saturate the magnetic moments of the Fe whisker and 6ML Fe layer. For ferromagnetic coupling the 6ML resonance peak moves towards the Fe whisker spin-manifold.

(b) The surface mode of Fe whisker is affected by the 6ML Fe layer through the exchange coupling. In this case the 6ML Fe layer acts as a source of the Fe whisker surface pinning. The slope of the frequency dependence of the surface resonance mode as a function of the applied dc field was used to determine both the ferromagnetic and the antiferromagnetic coupling. The measurements of the exchange coupling through Cr interlayers was so far mostly limited to the Cr thickness range of 10-16ML, see Fig.1. At this point our quantitative studies of the exchange coupling are not yet complete. More complete results will be presented at the time of the Meeting. However several conclusions can be reached already. In all growths we see strong short wavelength oscillations as was observed by the NIST and Philips groups. The antiferromagnetic coupling was in the studied thickness range always antiferromagnetic for the odd number of atomic layers (11, 13, 15). The exchange coupling appears to be ferromagnetic for even numbers of atomic layers (12,14,16). Studies using thick Cr interlayers are needed to determine quantitatively the strength of ferromagnetic coupling. The antiferromagnetic coupling at 15ML of Cr is  $.25 \text{ ergs/cm}^2$ . The antiferromagnetic coupling at 11ML of Cr is very strong. Even an applied external field of 10 kOe was not sufficient to line up the magnetic moments. The shift in the surface mode shows that the antiferromagnetic coupling reaches the value of  $\sim 1.3 \text{ ergs/cm}^2$ . The antiferromagnetic coupling in our samples is significantly stronger and the observed oscillations in the exchange coupling are significantly more pronounced than those observed by the Philips group. The above studies were carried out for samples in which the Cr interlayers were terminated at RHEED intensity maxima. Two samples which were terminated at RHEED intensity minima (13.5ML and 14.5ML), showed a strong antiferromagnetic coupling. Surprisingly the antiferromagnetic coupling in these samples is noticeably stronger than that corresponding to the closest odd number of atomic layers, see Fig1.

The Authors would like to thank the National Sciences and Engineering Research Council of Canada for grants supported this work. The Authors would like to thank

also Dr. A.S. Arrott for providing them with Fe whiskers and Dr. Z. Celinski and Mr. K. Myrtle for their help during this work.

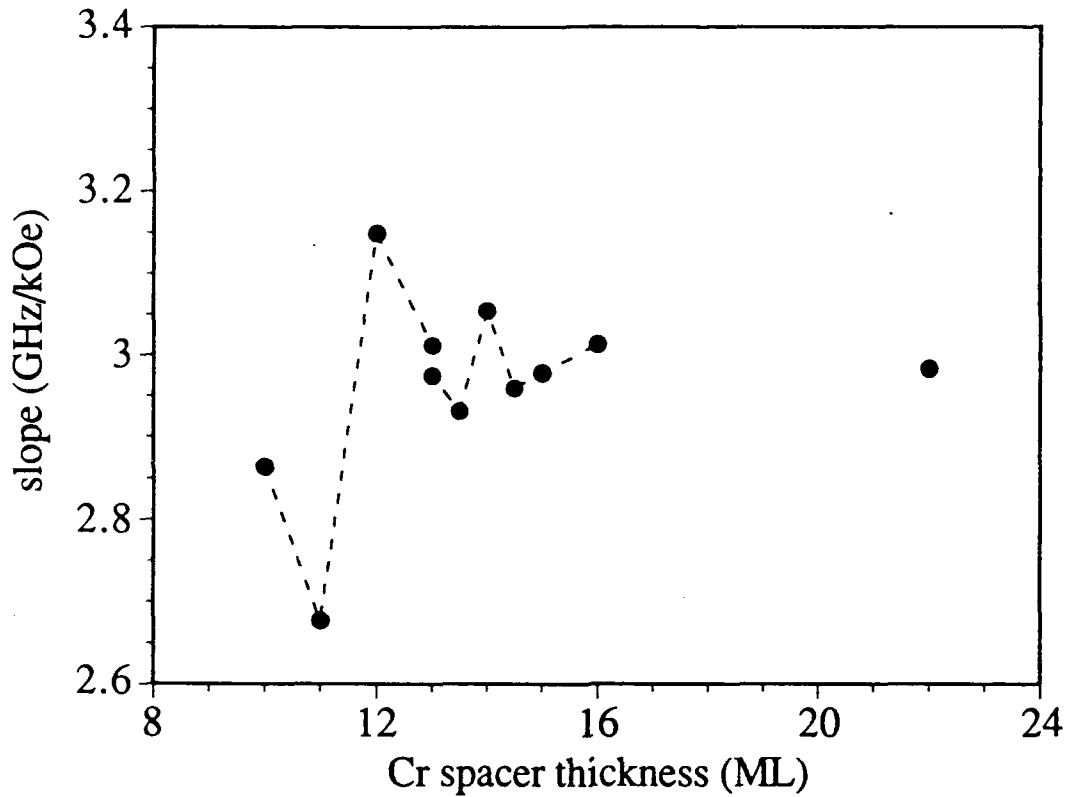


Fig.1: The slope of the resonance frequency of the Fe(001) whisker surface mode in [Fe(001) whisker/Cr(001)/6MLFe(001)/ 10MLAg(001)/20MLAu(001) samples as a function of Cr(001) interlayer thickness. The ferromagnetic coupling increases and the antiferromagnetic coupling decreases the slope of the surface mode respectively.